Design, Syntheses and Characterization of Multifunctional Organic-Inorganic Hybrid Materials

A Thesis submitted to

Indian Institute of Science Education and Research, Pune

In partial fulfilment of the requirements for the

MS Programme

Thesis Supervisor: Dr. Sujit K. Ghosh (IISER Pune)

By

Naveen Kumar

Registration No. 20111056

Chemistry Department

March, 2016

Indian Institute of Science Education and Research Pune,

900, NCL Innovation Park, Dr Homi Bhabha Road, Pune, Maharashtra 411008, India

Dedicated to my parents

CERTIFICATE

This is to certify that this dissertation entitled "**Design, Syntheses and Characterization of Multifunctional Organic-Inorganic Hybrid Materials**" towards the partial fulfilment of the MS programme at the Indian Institute of Science Education and Research, Pune represents original research carried out by Naveen Kumar at IISER Pune under the supervision of Dr. Sujit K. Ghosh, Associate Professor, Department of Chemistry during the academic year 2015-2016.

Naveen Kumar
Signature of student

Date 23/03/2016

Signature of supervisor

Date 23/03/2016

DECLARATION

I hereby declare that the matter embodied in the report entitled "**Design, Syntheses and Characterization of Multifunctional Organic-Inorganic Hybrid Materials**" are the results of the investigations carried out by me at the Department of Chemistry, IISER Pune, under the supervision of Dr. Sujit K. Ghosh and the same has not been submitted elsewhere for any other degree.

Naveen Kumar

Signature of student

Date 23/03/2016

ACKNOWLEDGMENT

Foremost, I would like to express my sincere gratitude to my mentor Dr. Sujit K. Ghosh for the continuous support offered throughout the tenure of the project. His mentorship was paramount in providing a well-rounded experience consistent my long-term career goals.

Besides my advisor, I would like to thank Dr. Christian Serre, research director of Institut Lavoisier de Versailles, UVSQ, Versailles (France) for his kind support and giving me chance to experience a 2.5 months research exposer in his lab and allowing me to add the carried research work to my thesis. Also, I would like to thank the rest of my thesis advisory committee for encouragement and insightful comments.

My sincere thanks also goes to Avishek Karmakar, who helped me throughout my thesis project. His guidance helped me in all the time of research and writing of this thesis. The thesis wouldn't be completed without the support and proper guidance of Dr. Clemence Sicard, an assistant professor at Institut Lavoisier de Versailles, UVSQ, Versailles (France). My hearty thanks goes to her also.

I thank my fellow lab mates: Sanjog Nagarkar, Biplab Joarder, Soumya Mukherjee, Biplab Manna, Aamod Desai, Partha Samanta, Shivani Sharma, Samraj Mollick, Yogeshwar More, Prateek Agrawal, Kriti Gupta, Arunabha Sen, Tarak Nath and Arif Inamdar for the stimulating discussions and for all the fun we had in the last couple of years.

My hearty thanks to my dear friends Agrim Saini, Alpesh Patil, Abhinav Sahni, Khushboo Singh and Ruchi Washnik for never making me feel research as boring and for being there every time whenever I needed.

Last but not the least; I would like to thank my family for all the love, assistance and guidance they have provided me throughout my life.

ABSTRACT

Multifunctional Metal-organic frameworks (MOFs) have been the theme of cutting edge research in the modern era. Because of diversified structures, structural tunability and targeted host-guest interactions in these porous architectures, MOFs have shown promising potential in terms of applicability in almost all spheres of material science. From the designing aspect, one of the key strategies is choice of ligands used in MOF syntheses. Neutral nitrogen donor ligands lead to formation of cationic frameworks resulting in the occupancy by extra framework anions for balancing overall charge of the frameworks. Such framework cations can often be exchanged with exogenous anions resulting in not only structural changes, but also visual colorimetric changes depending on the judicious choice of the metal centre such as Cu (II) ions. On the other hand Dicarboxylate based ligands are the most widely used ligands used in fabrication of such porous frameworks. Anionic carboxylate linkers not only give rise to robust and rigid MOFs but also in some cases flexible frameworks may result giving rise to multi-variant functionalities. From the application perspective if a MOF material can be down sized in Nano metric scale, then they can be efficiently used as mixed matrix membranes (MMMs) in conjunction with organic polymers for addressing one of the key global problems i.e. separation of CO_2 from other gases. Bearing this in mind, my thesis work pivots around design, syntheses and characterization of two metal-organic hybrid materials for a) naked eye colorimetric anion sensing b) development of MOF based MMMs for CO_2 separation.

CONTENTS

LIST OF FIGURES

Chapter 1

Chapter 2

LIST OF TABLES & SCHEMES

Chapter 1

Chapter 2

Chapter 1

Design, Synthesis and Characterization of a Metal-Organic Coordination polymers for selective colorimetric anion exchange

Introduction

Metal organic frameworks (MOFs) or porous co-ordination polymers (PCPs), comprising of metal ions and bridging organic struts have attracted the scientific community a lot in last two decades.[1] Due to their hybrid nature, possessing porous channels and tuneable framework size & functionality, they show diversified applications like gas storage & separation, catalysis, sensing, drug delivery, proton conduction and anion exchange.[2]

Guest responsive dynamism in MOFs has caught immense attention in recent past.[3] Such MOFs show guest inclusive structural behaviour with the change in chemical environment (Fig. 1). Guest responsive structural dynamism is an important aspect in such cases as the structure can be tuned in accordance to a change in any physical or chemical stimuli (Fig. 2). In the recent past, cationic frameworks has been known to be one of the prime candidates to show structural dynamism.[4] The cationic MOFs are generally comprised of metal cations and neutral ligands with the extra framework anions present inside the structural voids or weakly co-ordinated to the metal ions. Although there are several other ways to construct cationic frameworks (Fig. 3), using neutral ligands for fabrication of cationic frameworks still remain one of the main standard protocol for generating cationic frameworks.[5] The charge balancing framework anions could be exogenously exchanged with other foreign anions of different shape, size and co-ordination tendency. Since very often, the exchanged anions are of different shapes, sizes and coordinating tendency, exchange properties lead to changes in the overall framework due to inherent flexibility of such cationic frameworks.[6] The residing anions are weakly or strongly hydrogen bonded to the framework lattice and thereby exchange by foreign anions resultig in structural changes in the framework lattice. Also, due to the presence of large guests inside the porous channels of such cationic frameworks, they are perhaps, the best manifestations of guest induced structural transformation.[7] Anion sensing and recognition has its own importance, because of its involvement in several of chemical and biological processes.[8] The anion exchange phenomenon can be either monitored by spectroscopic techniques or by a much simpler way by visual chroma. However, the naked eye detection without any spectroscopic

techniques dominates over other sensing techniques, because of its ease in the detection methods.[9]

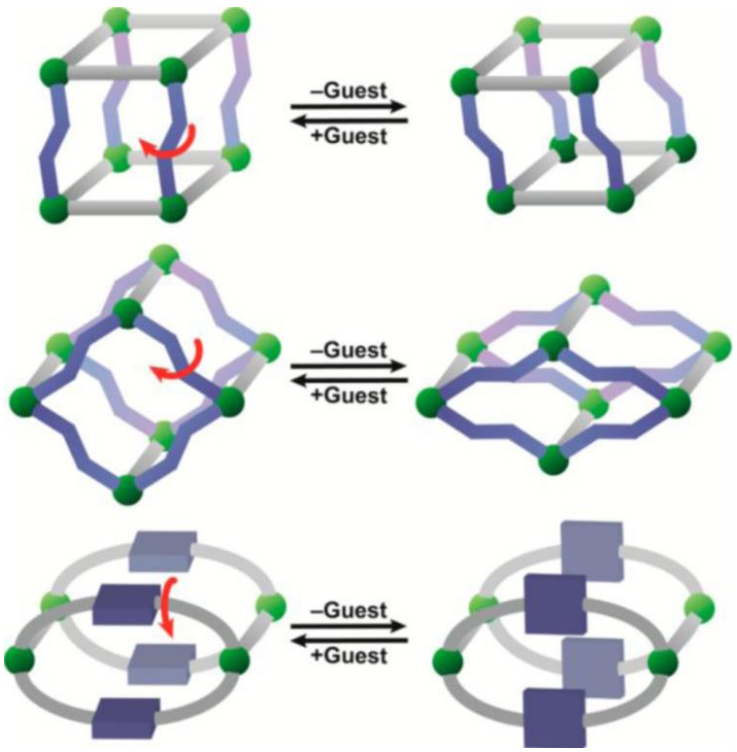

Figure 1. Guest induced structural transformation in flexible frameworks.[10]

Cationic MOFs involving Cu (II) as the metal centre are known to be the suitable candidate to fabricate colorimetric anion sensors.[11] The Cu (II)-complexes involve

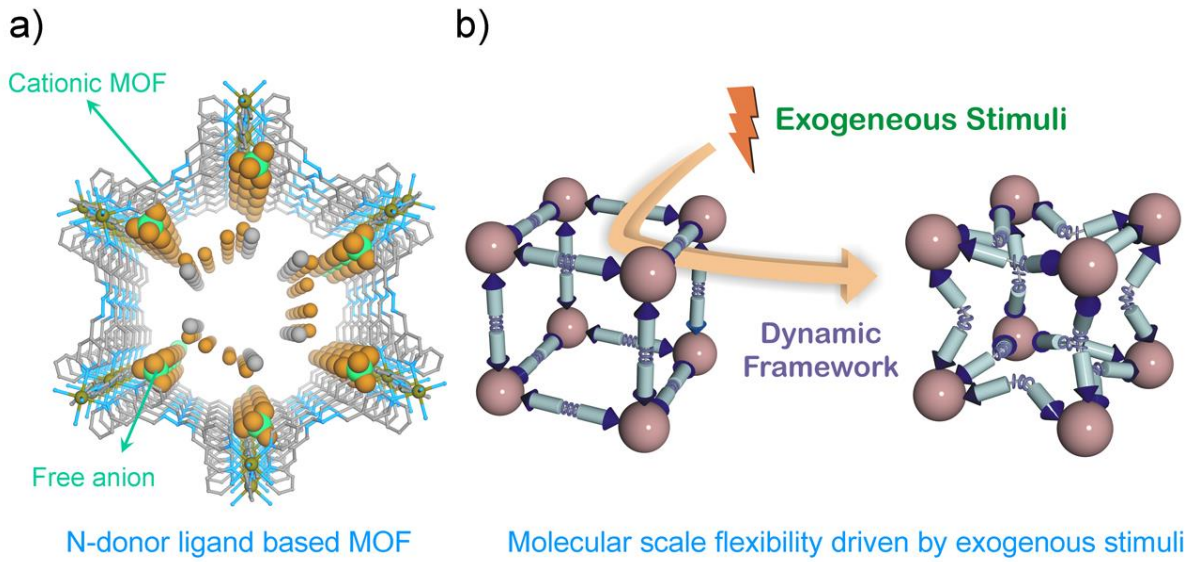

Figure 2.a) Cationic MOF showing free anions in porous channels and b) Stimuli driven structural transformation in flexible frameworks.[12]

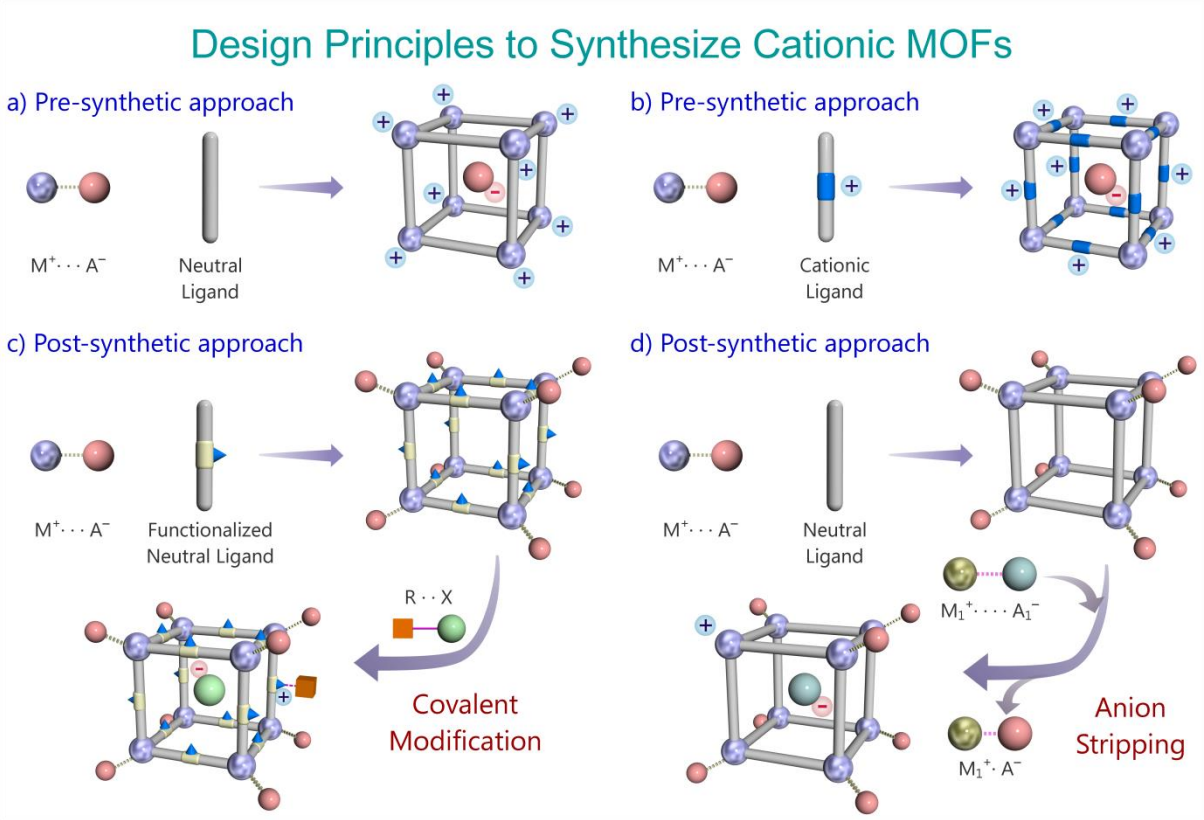

Figure 3. Synthetic approach to fabricate cationic MOFs.[13]

anions of different size, shape and co-ordination ability. Such complexes exhibit colour change, while exchanged with different anions because of Jahn-Teller distortions caused by the weakly co-ordinated anions at the axial positions. The anions at the axial positions could be easily exchanged by other foreign incursive anions resulting in colorimetric changes. In a classical report by Bu et al. a novel cationic framework based on Cu (I) and a neutral N-donor ligand was synthesized, which harboured free nitrate anions in its porous channels. The free anions were exchanged with foreign anions like F^-, Cl^-, Br^-, I^-, N_3^-, SCN^-, CO_3^{2-} to give remarkable visual changes to the colour of the pristine compound (Fig. 4-a). In an another report from our group, a one-dimensional framework based on Cu (II) and a neutral amide based ligand was synthesized. The nitrate anions were coordinated to the axial positions of the metal centre which could be exchanged with a linear anion like SCN^- resulting in colorimetric changes (Fig. 4-b).

Carbon dioxide gas capture and separation from the mixture of gases is industrially important and necessary to diminish the effects of global warming.[14] Flue gases emanating from the industries are the major source of anthropogenic CO_2 emission, caused by burning of fossil fuels. Based on CO_2 generation, three major processes have been developed to capture CO_2 from the flue gases: 1) pre-combustion capture, 2) post-combustion capture and 3) oxyfuel combustion capture.[15] Pre-combustion capture and oxyfuel combustion capture involve high capital costs, for production of H_2 gas and requirement of pure O_2 gas in pre-combustion capture and oxyfuel combustion capture respectively. Post-combustion capture is the most efficient and feasible method. However, the post-combustion capture involves the

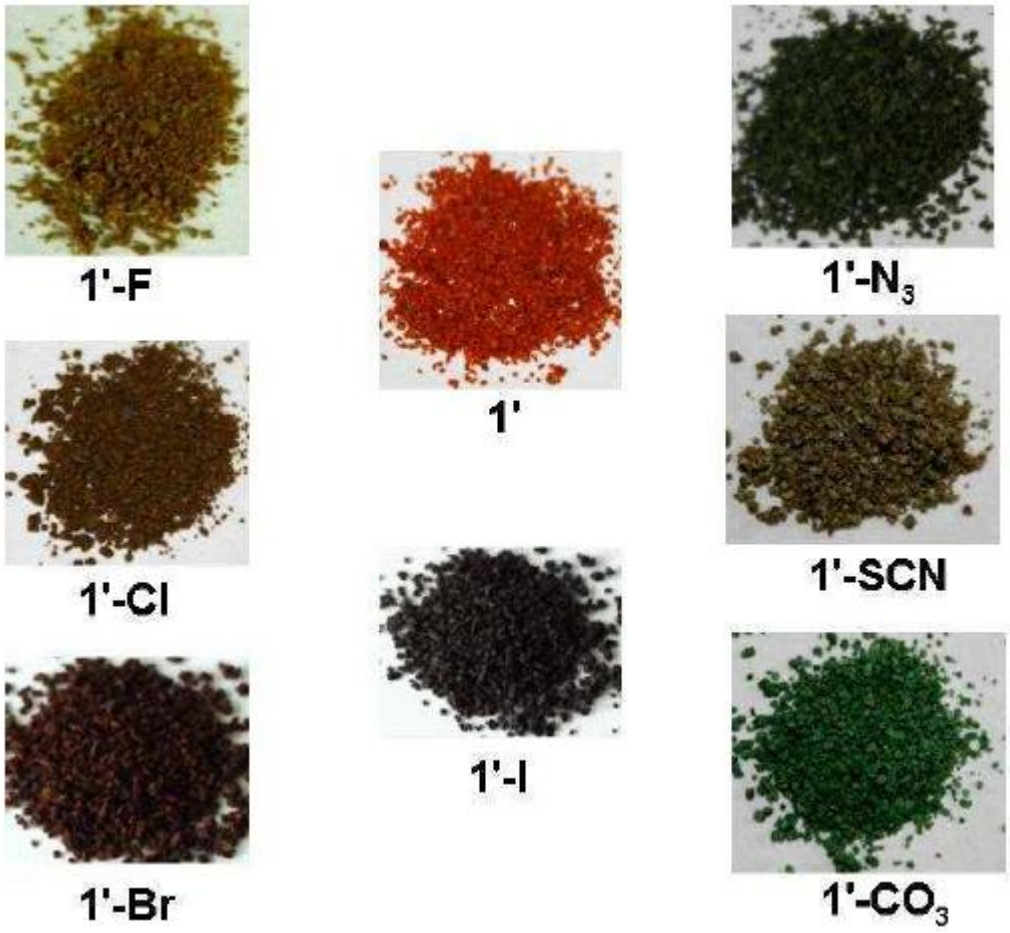

Figure 4.a) Illustration of colorimetric anion exchange involving copper metal ion[16].

mixture of CO_2 and N_2 gases. Hence, for the effective capture of CO_2, it needs to be separated from mixture of CO_2 and N_2 gases. There have been many MOFs reported in the literature having the potential to capture and separate CO_2 selectively from CO_2 and N_2 mixtures.[17]

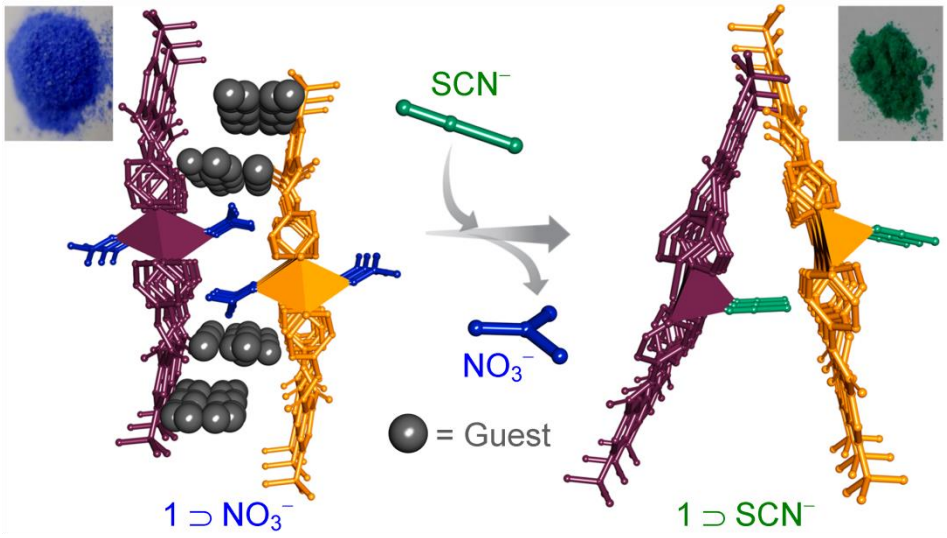

Figure 4.b) Structural dynamism accompanied by colorimetric anion exchange.[18]

Herein, we report a 1-D coordination polymer, based on a neutral N-donor ligand and a Cu (II) metal ion. The resulting cationic framework harbours free BF_4^- anions inside the porous channels and also coordinated BF_4^-anions to the metal centre. These anions could be exchanged exogenously with both weakly coordinating anions like NO_3^-, ClO_4^- and strongly coordinating anions like N_3^-, SCN^- anions, both resulting in colorimetric changes accompanied by structural changes in the framework. The parent compound also showed guest dependent structural changes resulting in the formation of an air dried phase. The air dried phase also showed a selective uptake of CO_2 over N_2 due to the presence of lewis basic sites in the framework. Such a multifunctional behaviour in CPs are a rare phenomenon and if achieved economically holds great promise for the future for the fabrication of new materials.

Experimental Section

Materials: All the chemicals used are commercially available and were used as it, without any further purification.

PHYSICAL MEASUREMENTS:

- **Powder X-ray Diffraction (PXRD)**: We measured all the PXRD patterns on Bruker D8 Advanced X-Ray Diffractometer at room temperature using Cu-Kαradiation (1.5406 Å) at a scan speed of 0.5° min^{-1} and the step size of 0.01° in 2 theta.

- **Thermogravimetric analysis (TGA):** All TGA data were recorded on the Perkin-Elmer STA 6000, TGA analyser under N_2 atmosphere with the heating rate of 10°C min^{-1}.

- **Infra-Red Spectroscopy (IR):** All the Infrared spectra were recorded on the Thermo-scientific–Nicolet-6700 FT-IR spectrometer. The FT-IR spectra were recorded using KBr Pellets with a very amount of the respective samples.

- **UV spectroscopy**: The UV-Vis measurements were performed using Chemito SPECTRASCAN UV-2600.

- **FE-SEM:** The EDX analysis and SEM image was obtained using FEI Quanta 3D dual beam ESEM at 30 KV.

- **GAS ADSORPTION:** Gas adsorption measurements were studied using the BelSorp-max instrument from Bel-Japan.

Single-crystal X-Ray Structural Studies:

We collected the single-crystal X-ray data of compound **1⊃BF_4^-** at 150(2) K on a Bruker KAPPA APEX II CCD Duo diffractometer (which was operated at 1500 W power: 50 kV, 30 mA) with the use of the graphite-monochromatic Mo Kα radiation (λ= 0.71073 Å). The single crystal was on the nylon Cryo-loops (Hampton Research) with Paraton-N (Hampton Research). We processed the integration and reduction of the data with the help of SAINT[19] software. We applied a multi-scan absorption correction to the collected reflections. We solved the structure by the direct method using SHELXTL[20] and refined on F^2 by full-matrix least-squares technique using the SHELXL-97[21] program package with the help of the WINGX[22] programme. We refined all non-hydrogen atoms anisotropically. We located the all hydrogen atoms in successive difference Fourier maps and then we treated them as riding atoms using SHELXL default parameters. We examined the structures using the Adsym subroutine of PLATON[23] to assure that no additional symmetry could be applied to the models.

Ligand (L) Synthesis:

Synthetic procedure:

Ligand L was synthesized following the previously reported procedure (scheme 1).[24] Cyanuric chloride (1 g, 5.42 mmol) was added to the 30 ml pressure tube, followed by the addition of imidazole (2.22 g, 32.53 mmol) without any solvent. The reaction mixtures

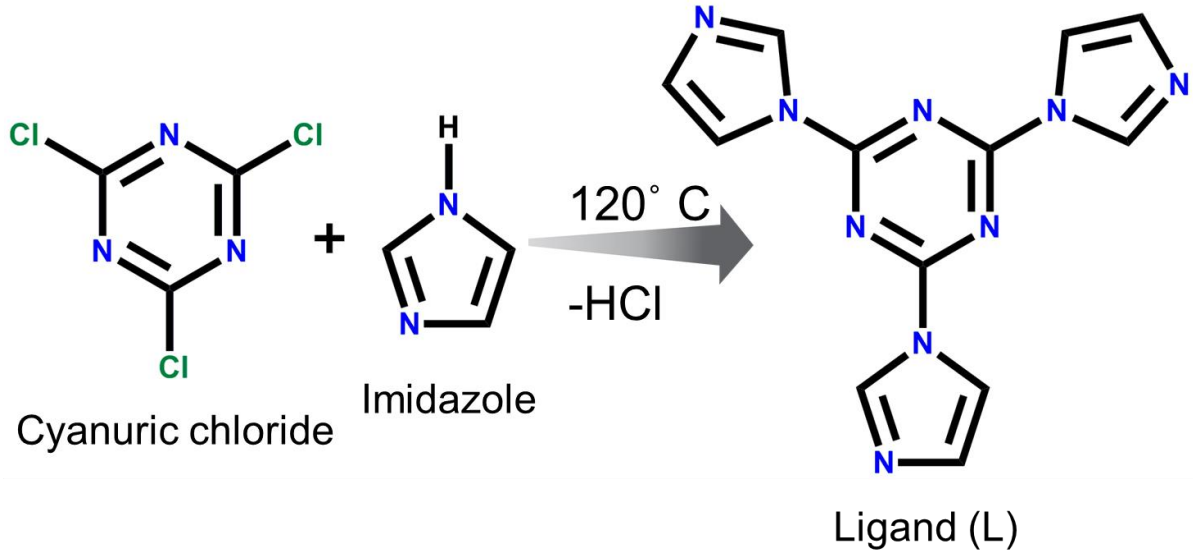

Scheme 1: Synthetic scheme for the preparation of ligand **L**.

were reacted for about 2 hours at 120°C. Then the product was extracted using the 1000 ml separating funnel, collecting the organic layer in chloroform (100 ml) and inorganic layer in water (100 ml). The chloroform layer was collected separately and the water layer was extracted further with chloroform (4 X 100 ml). All the chloroform layers were separated collectively and washed with brine solutions (2 X 100 ml). The washed organic layer was dried over sodium sulphate and white colour compounds (L) were obtained evaporating the chloroform. Formation of the ligand L was confirmed by HRMS (High Resolution Mass Spectroscopy) (figure 5) and ^{1}H &^{13}C NMR (figure 6.a & 7.b).

HRMS: Calculated mass $(L + H)^{+}$ = 280.1059, mass obtained = 280.1058.

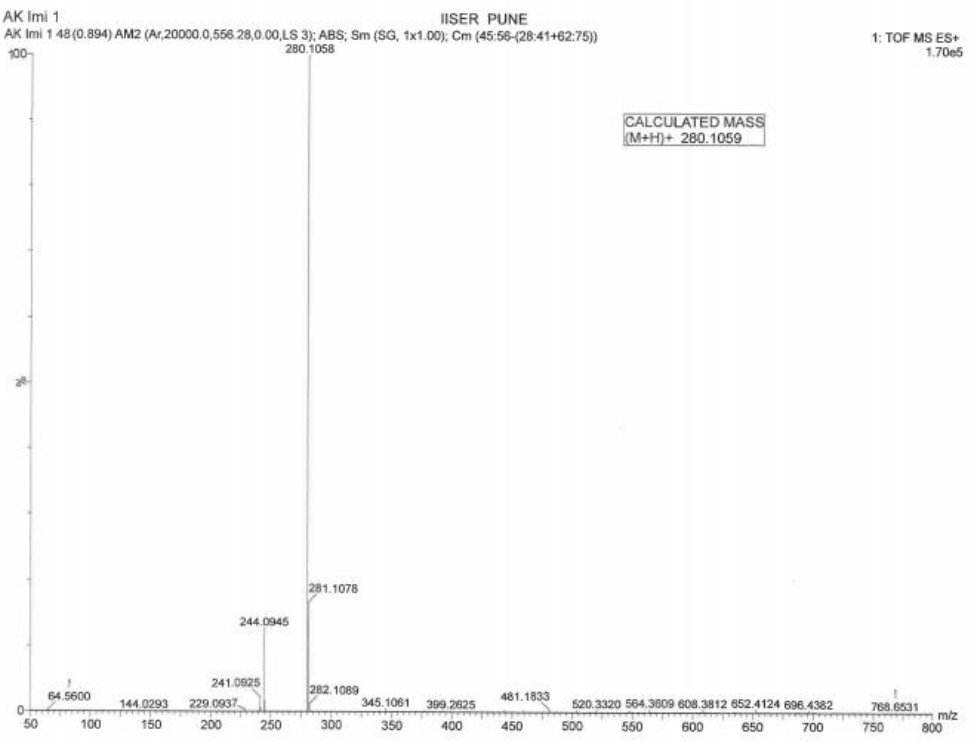

Figure 5. HRMS spectra of the ligand L.

Proton NMR (^{1}H):

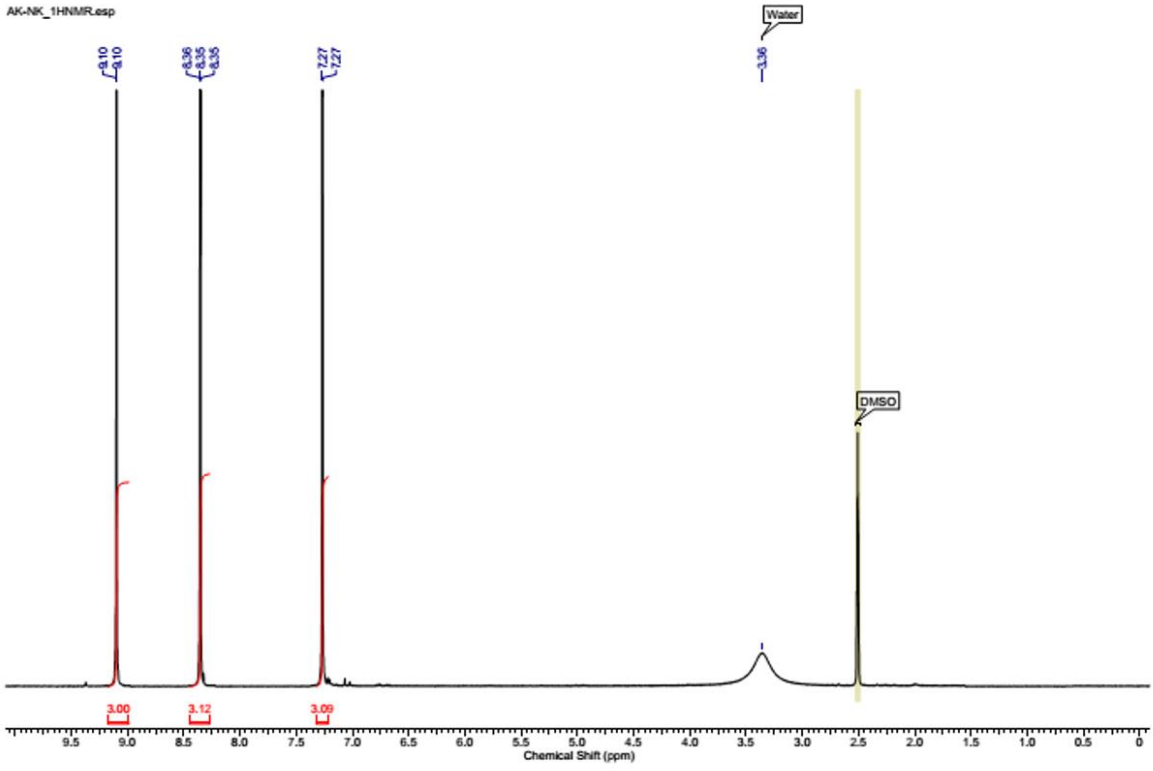

Figure 6.a) Proton NMR (^{1}H) of the ligand L.

^{13}C NMR:

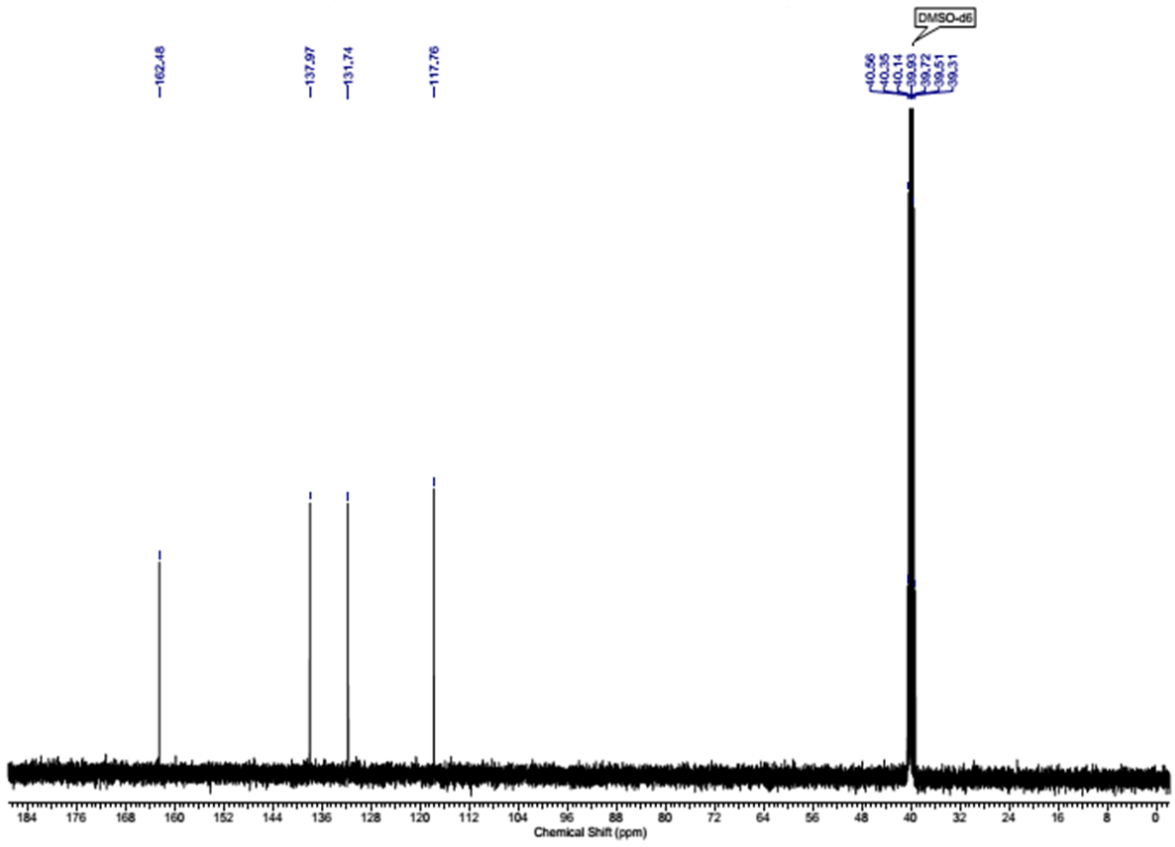

Figure 6.b) ^{13}C NMR of the ligand L.

Synthesis of the Compound 1⊃BF_4^-: [{(Cu)(**L1**)$_2$(MeOH)(BF_4)}.(BF_4).xG]$_n$

Before finalising the synthetic procedure of the co-ordination polymer, we attempted several combinations of metals salts, solvents and the ligand **L**, and several synthetic procedures like hydrothermal, solvothermal and slow diffusion & evaporation crystallisation technique. The compound **1⊃BF_4^-** was synthesized following the slow diffusion and evaporation crystallization technique at room temperature (scheme 2). 1 ml of DCM solution of the ligand **L** (14 mg, 0.05 mmol) was added to a 6 mm glass tube. 1 ml of p-Xylene was layered on the top of DCM solution and finally 1 ml of MeOH solution of the metal salt Cu(BF_4)$_2$.6$H_2$0 (11.8 mg, 0.05 mmol) was added at the top most layer. Blue coloured perfect single crystals were obtained after 5 days. The structure of the compound **1⊃BF_4^-** was obtained by single-crystal X-ray diffraction technique. The parent compound upon exposure to air changed to a new phase **1′⊃BF_4^-** due to partial loss of solvent guest molecules from the framework.

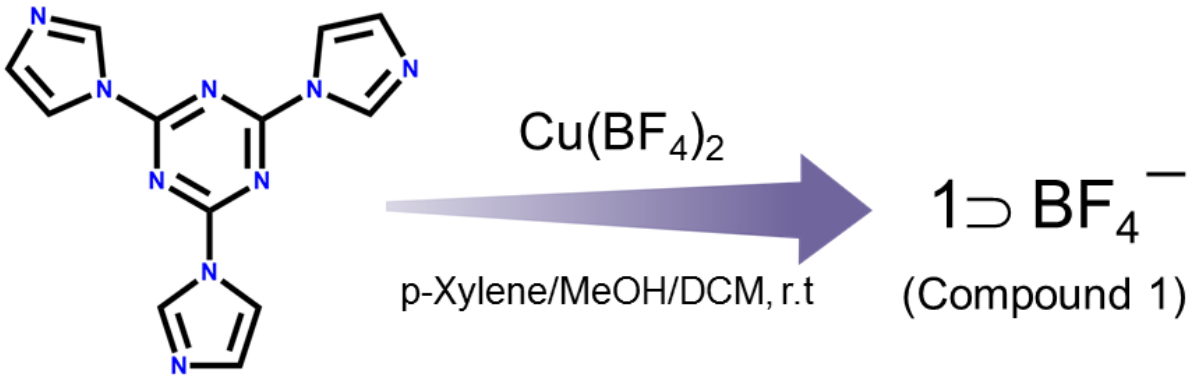

Scheme 2: Synthetic scheme for the preparation of Compound 1.

However as reported earlier in literature, we observe that during complex formation the ligand underwent a significant transformation due to hydrolysis and gets modified to form a new ligand L1 as shown in Scheme 3.

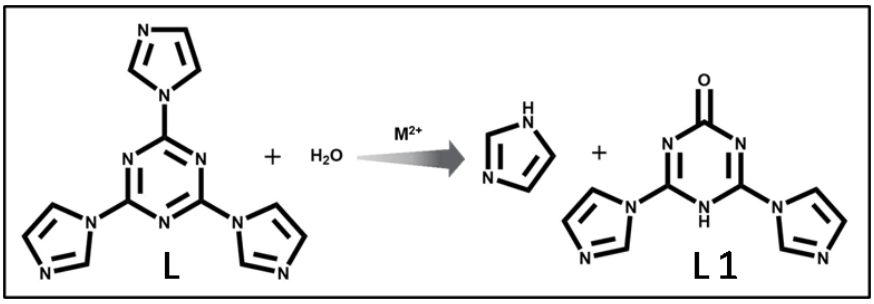

Scheme 3: Ligand modification resulting in the formation of L1 during complexation.[25]

ANION EXCHANGE STUDIES:

The blue coloured air dried crystalline compound **1′⊃BF_4^-** (10 mg) was stirred very slowly in 5 mL of MeOH solutions containing 0.1 mmol of KSCN, $NaNO_3$, $NaClO_4$ and 0.05 mmol of NaN_3in 15 ml glass vials separately for about 4 days at room temperature which to get the anion exchanged product. The anion exchanged products were characterized by FT-IR, PXRD&UV spectroscopy.

ANION SELECTIVITY TEST:

Separation of N_3^- and SCN^-:

The blue coloured air dried crystalline compound **1′⊃BF_4^-** (10 mg) was stirred very slowly in 5 mL of MeOH solutions containing equimolar NaN_3 (0.05 mmol) and KSCN (0.05 mmol) in a 15 mL glass vial for about 4 days at room temperature to get the anion exchanged product, which was further characterized by FT-IR spectra.

Separation of SCN^- and NO_3^-:

The blue coloured air dried crystalline compound **1′⊃BF_4^-** (10 mg) was stirred very slowly in 5 mL of MeOH solutions containing equimolar KSCN (0.1 mmol) and $NaNO_3$ (0.1 mmol) in a 15 mL glass vial for about 4 days at room temperature to get the anion exchanged product, which was further characterized by FT-IR spectra.

Separation of SCN^- and ClO_4^-:

The blue coloured air dried crystalline compound **1′⊃BF_4^-** (10 mg) was stirred very slowly in 5 mL of MeOH solutions containing of equimolar KSCN (0.1 mmol) and $NaClO_4$ (0.1 mmol) in a 15 mL glass vial for about 4 days at room temperature to get the anion exchanged product, which was further characterized by FT-IR spectra.

Separation of N_3^- and ClO_4^-:

The blue coloured air dried crystalline compound **1′⊃BF_4^-** (10 mg) was stirred very lowly in 5 mL of MeOH solutions containing equimolar NaN_3 (0.05 mmol) and $NaClO_4$ (0.05 mmol) in a 15 mL glass vial for about 4 days at room temperature to get the anion exchanged product, which was further characterized by FT-IR spectra.

Separation of N_3^- and NO_3^-:

The blue coloured air dried crystalline compound **1′⊃BF_4^-** (10 mg) was stirred very lowly in 5 mL of MeOH solutions containing equimolar NaN_3 (0.05 mmol) and $NaNO_3$ (0.05 mmol) in a 15 mL glass vial for about 4 days at room temperature to get the anion exchanged product, which was further characterized by FT-IR spectra.

Separation of NO_3^- and ClO_4^-:

The blue coloured air dried crystalline compound **1′⊃BF_4^-** (10 mg) was stirred very slowly in 5 mL of MeOH solutions containing equimolar NaN_3 (0.1 mmol) and $NaClO_4$ (0.1 mmol) in a 15 mL glass vial for about 4 days at room temperature to get the anion exchanged product, which was further characterized by FT-IR spectra.

Results and Discussions

Single crystal X-ray diffraction analysis of compound 1⊃BF_4^- revealed that the compound crystallized in *Monoclinic* system with space group *P-1*. A minute examination of the structure illustrated that there are two types of copper centers in the parent compound. The asymmetric unit of the compound contain two copper ions, two ligands, one coordinated BF_4^- ion and one free BF_4^- ion, one methanol molecule coordinated to the copper centre and half p-xylene guest molecules (Fig. 7). One hexa-ligated copper atom is coordinated by nitrogen atoms of the imidazole unit from four ligands and the two BF_4^- ions which satisfy the coordination geometry. The other copper centre is coordinated by four imidazole nitrogen of the ligand and the other two sites are occupied by the methanol molecules resulting in octahedral geometry. Since a neutral N-donor ligand was used, free non-coordinating BF_4^- were observed in the framework lattice to balance the overall charge of the cationic framework. These two types of copper centre result in a zig-zag arrangement of 1D chain with p-xylene guest molecules, occupying the cavity of such 1D framework. $[\{(Cu)(\mathbf{L1})_2(MeOH)(BF_4)\}.(BF_4).xG]_n$ gives the structural formula of the compound 1⊃BF_4^-.

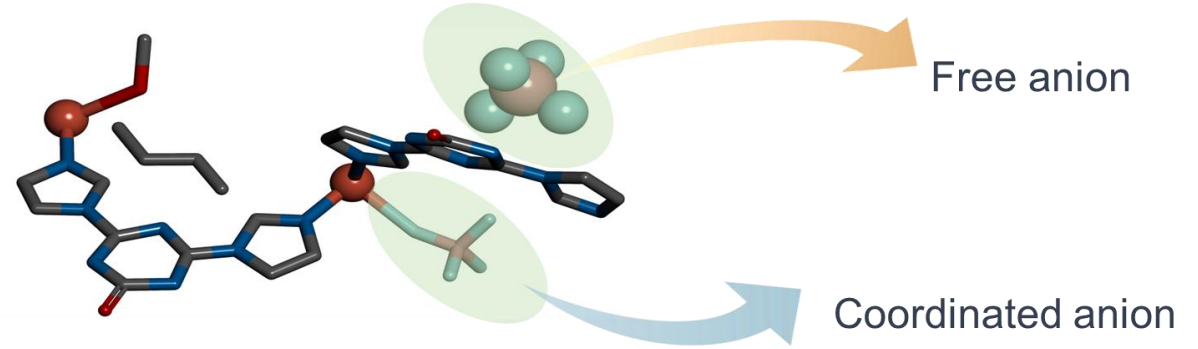

Figure 7. Asymmetric unit of compound 1⊃BF_4^-.

Interestingly, we speculate that when the parent compound was brought out of the mother liquor, the solvent guest molecules escape from the framework resulting in the formation of a new phase 1′⊃BF_4^-. Such type of dynamic behavior in 1D cationic CPs is quite commonly known in literature.[25] The Thermogravimetric analysis of compound 1′⊃BF_4^-showed a thermal stability up to ~220˚C with about 2-3% loss due to the solvent guest molecules (Fig. 11). However, when activated by critical point dryer using liquid CO_2, the solvent molecules are replaced by 2-Propanol thereby showing only

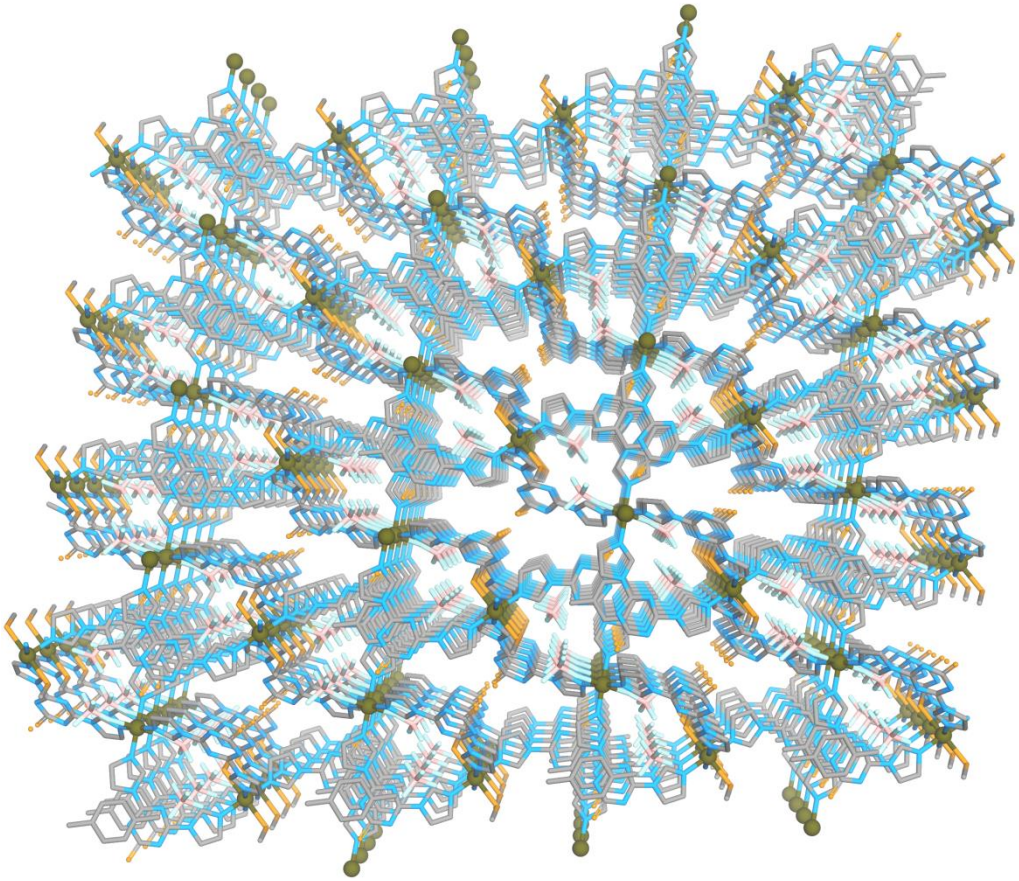

Figure 8. Packing diagram of compound 1⊃BF_4^- in perspective view.

a slight loss initially due to the replaced solvent molecules. The coordinated MeOH molecules are lost immediately upon exposure to air, thereby resulting in one of the

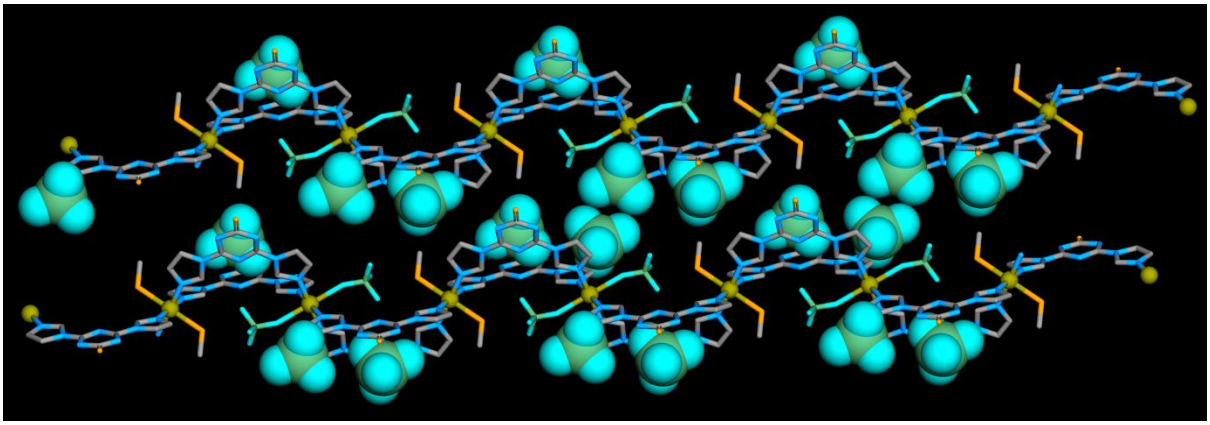

Figure 9. 1D chain of $1\supset BF_4^-$ showing coordinated anions and free anions .

copper centre in the framework adopting a tetrahedral geometry. In view of the presence of both coordinated and free BF_4^- ions in the framework, we resorted in performing anion exchange experiment using the protocol as mentioned before. For these we chose two types of anions a) weakly or non-coordinating anions like NO_3^-, ClO_4^- ions and moderately/ strong coordinating anions like SCN^- or N_3^- anions (Fig. 10).

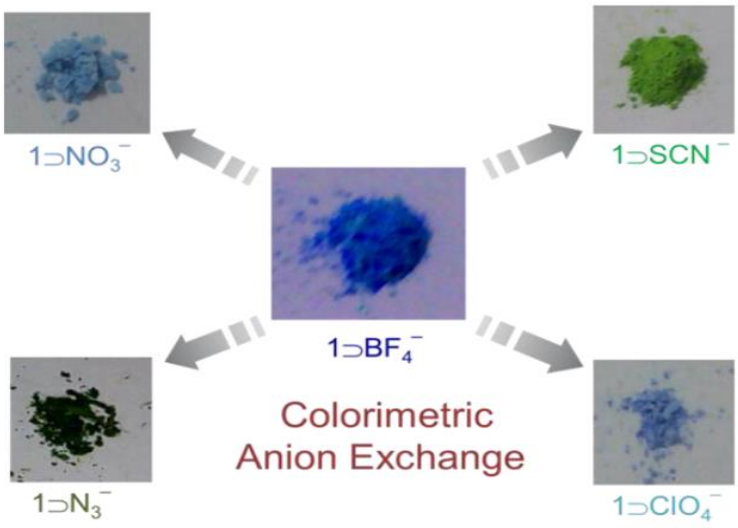

Figure 10. Colorimetric changes occurring in case of strongly coordinating anions whereas subtle changes occurring in case of weakly coordinating anions.

As evidenced from the IR spectra of the anion exchanged products, the peaks for BF_4^- (1120cm^{-1}) ions in the parent compound i.e. 1'⊃BF_4^- are almost absent in the exchanged compounds, whereas new peaks for NO_3^- (1380cm^{-1}), ClO_4^- (1080cm^{-1}), SCN^- (2050cm^{-1}), N_3^- (2100cm^{-1}) appear, which confirms the anion exchange process (Fig. 13). Interestingly, for strongly coordinating anions like SCN^- and N_3^- we observed a visual colorimetric change accompanying the anion exchange phenomenon (Fig. 10). This can be corroborated to the fact that in such case, the incoming foreign anions replace the coordinated BF_4^- anions from the metal centre owing to their strongly coordinating nature, hence resulting in such color changes. Due to Jahn-Teller Distortion at the axial positions of the copper centre, the Cu-BF_4^- bond is significantly weakened and therefore can be easily replaced by anions of linear geometry resulting in colorimetric changes. For weakly coordinating anions like NO_3^- and ClO_4^-, we expect that the interstitial free anions are exchanged and thereby no

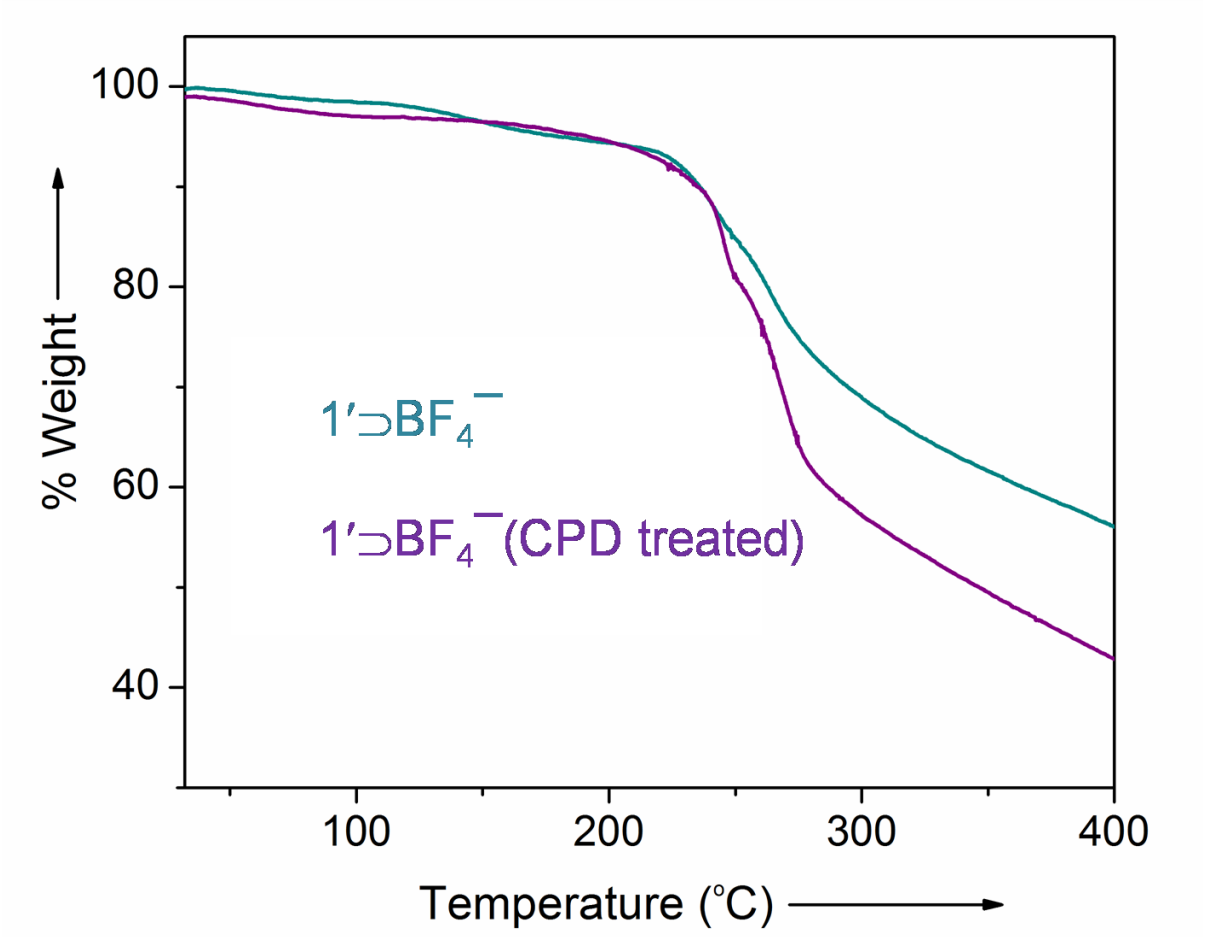

Figure 11. TGA profile of compound 1′⊃BF_4^- (violet) and CPD treated 1′⊃BF_4^- (dark cyan).

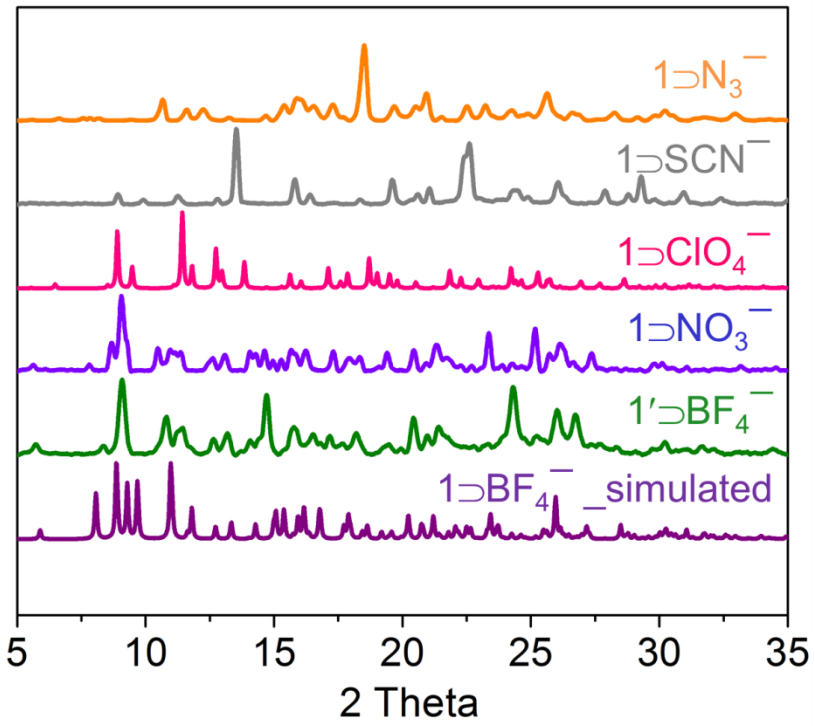

Figure 12. PXRD pattern of the 1′⊃BF_4^- and other anion exchanged samples.

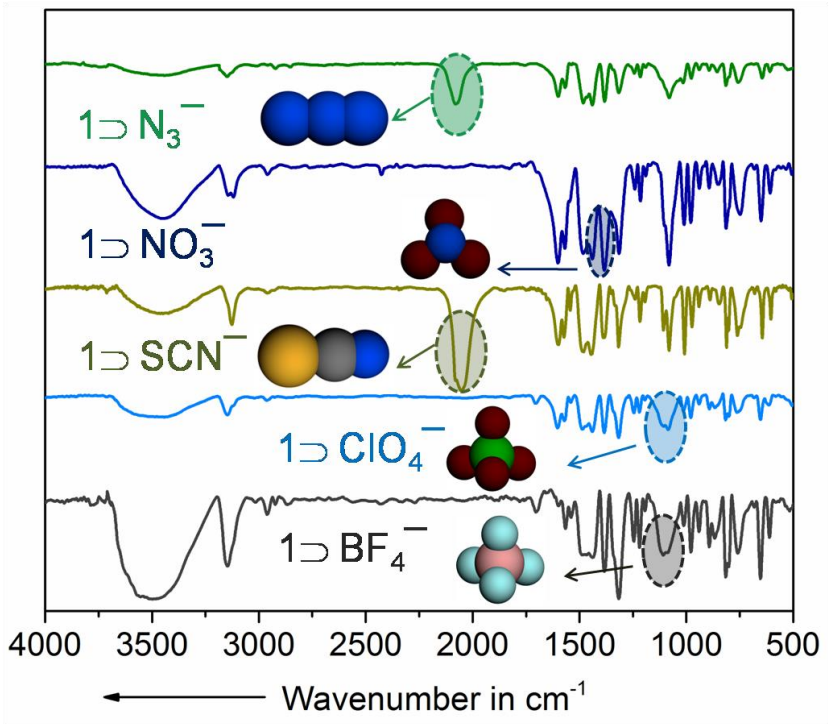

Figure 13. IR spectra of compound 1⊃BF_4^- and other anion exchanged compounds

subsequent changes in the colour are observed. The PXRD patterns of the anion exchanged samples reveal structural transformation owing to different shape and size of the incoming anions (Fig. 12). For weakly coordinating/ non-coordinating

anions we see that the PXRD patterns being quite similar to the parent compound 1'⊃$BF_4^-$with subtle changes in the pattern. However, for strongly coordinating anions we observe a similar trend in the PXRD patterns correlating to the fact that the framework being dynamic adjusts in such a way to accommodate the incoming foreign anions. The dynamic anion exchange process in flexible cationic frameworks has been reported previously by our groups and some other groups around the world. For any anion exchange process involving multiple anions, it is imperative to determine the affinity of anion in order to determine the order of anion exchange. In a typical experimental protocol as described before, equimolar concentration of anions of six different combinations were used to check the affinity order viz. SCN^-/ NO_3^-, N_3^-/ SCN^-, SCN^-/ ClO_4^-, N_3^-/ ClO_4^-, N_3^-/ NO_3^-, NO_3^-/ ClO_4^-. It was observed that with the combinations of weakly coordinating anions and strongly coordinating anions like SCN^-/ NO_3^-, SCN^-/ ClO_4^-, N_3^-/ $ClO_4^-$and N_3^-/ NO_3^- only strongly coordinating

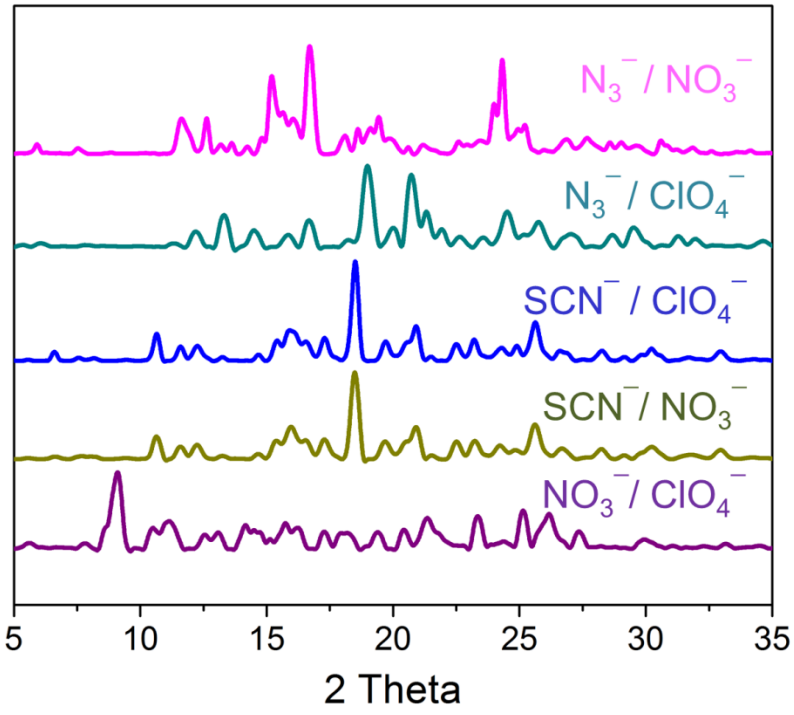

Figure 14. PXRD of anion exchanged samples in binary combination to check the affinity.

anions i.e. N_3^- and SCN^- were preferentially exchanged (Fig. 15-17). This may be due to the stronger coordinating power and also the linear geometry of the incoming anions.

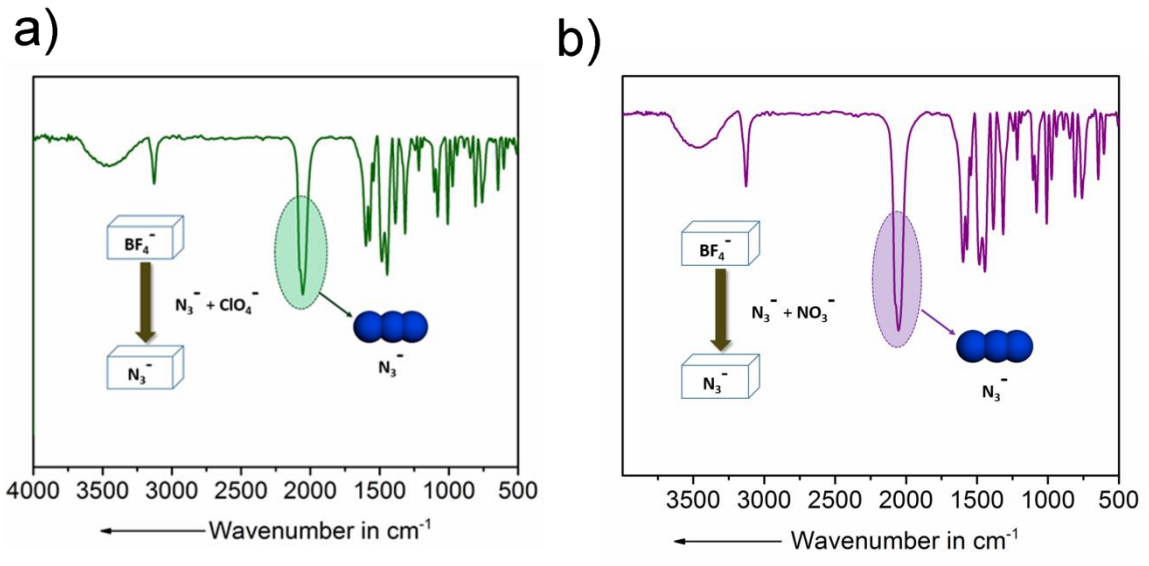

Figure 15. FT-IR spectra of binary combinations: a) N_3^- /ClO_4^- and b) N_3^- / NO_3^-

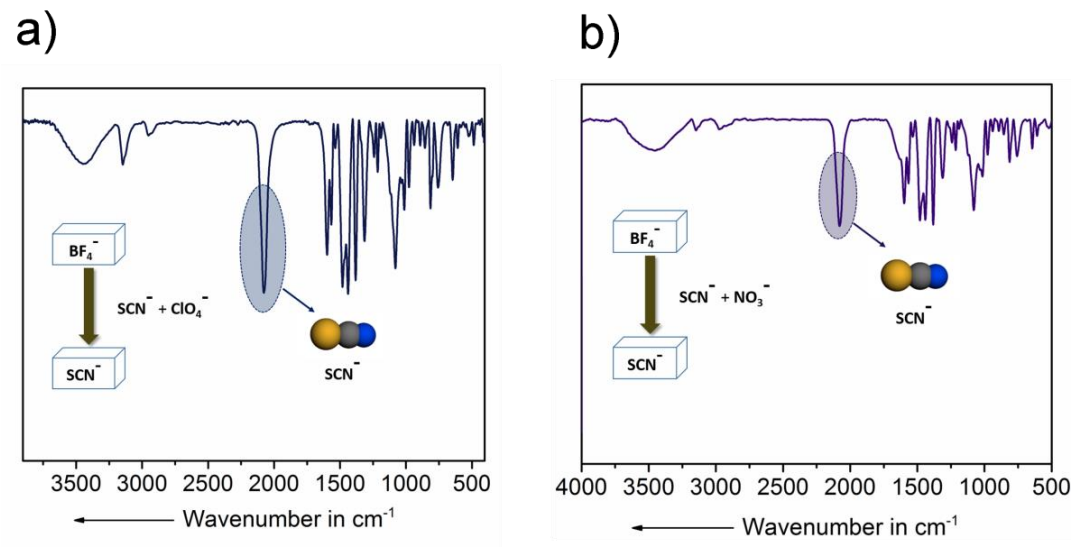

Figure 16. FT-IR spectra of binary combinations: a) SCN^- / $ClO_4^-$and b) SCN^-/ NO_3^-

From the mixture of NO_3^-/ ClO_4^-, $NO_3^-$was preferentially taken owing to the fact that nitrate anions are smaller in size than the perchlorate anions. Whereas amongst the combination of N_3^-/ SCN^-, N_3^- ion was selectively taken. These results prove the fact that both the coordinating ability and size of the incoming guest anion play a crucial role in such preferential exchange phenomenon. From the above results we estimate that the affinity order for such anion exchange process is N_3^->SCN^->NO_3^->ClO_4^-. The PXRD pattern of the corresponding anion exchanged samples in binary combinations is quite similar to the individual anion exchanged ones correlating to affinity order (Fig.14). Such type of preferential uptake of anions plays a crucial role in anion separation and may play a crucial role in anion exchange

membranes in industries. The SEM images of the anion exchanged samples also show a similar trend (Fig. 19). For non-coordinating anions, we observe a similar crystalline morphology whereas for strongly coordinating anions we observe a different morphology. The EDX results are also in good agreement with the anion exchange processes occurring herein (Fig. 20-24).

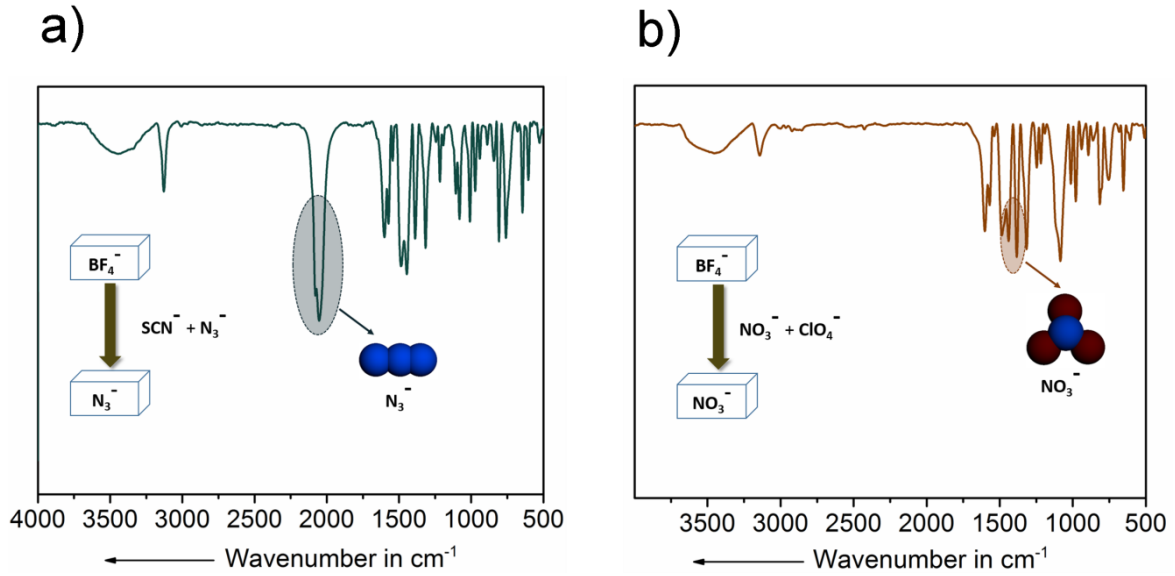

Figure 17. FT-IR spectra of binary combinations: a) N_3^-/ SCN^- and b) NO_3^-/ ClO_4^-.

Disperse phase UV experiments using acetonitrile as a solvent (fig. 18) revealed that in the anion exchanged samples, a shoulder peak around 280 nm appears, which is not present in the assynthesized compound.

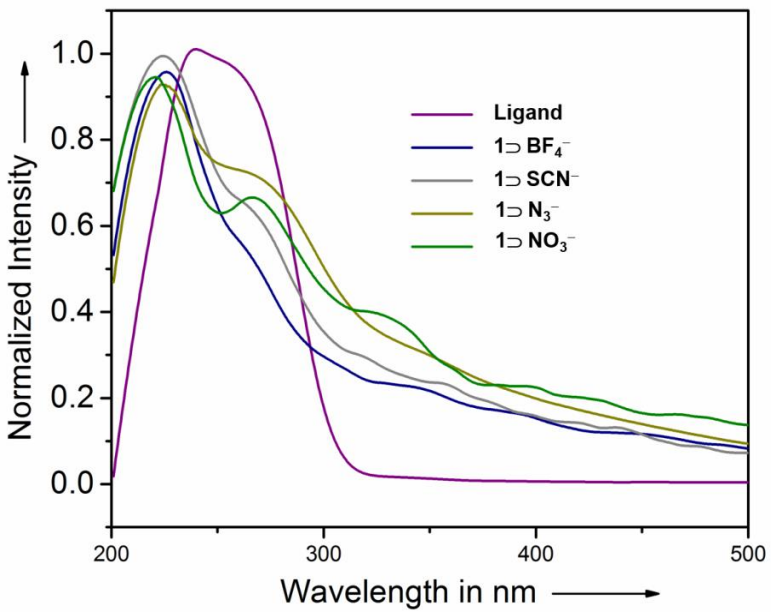

Figure 18. UV-Vis spectra of $1\supset BF_4^-$ and other anion exchanged compounds.

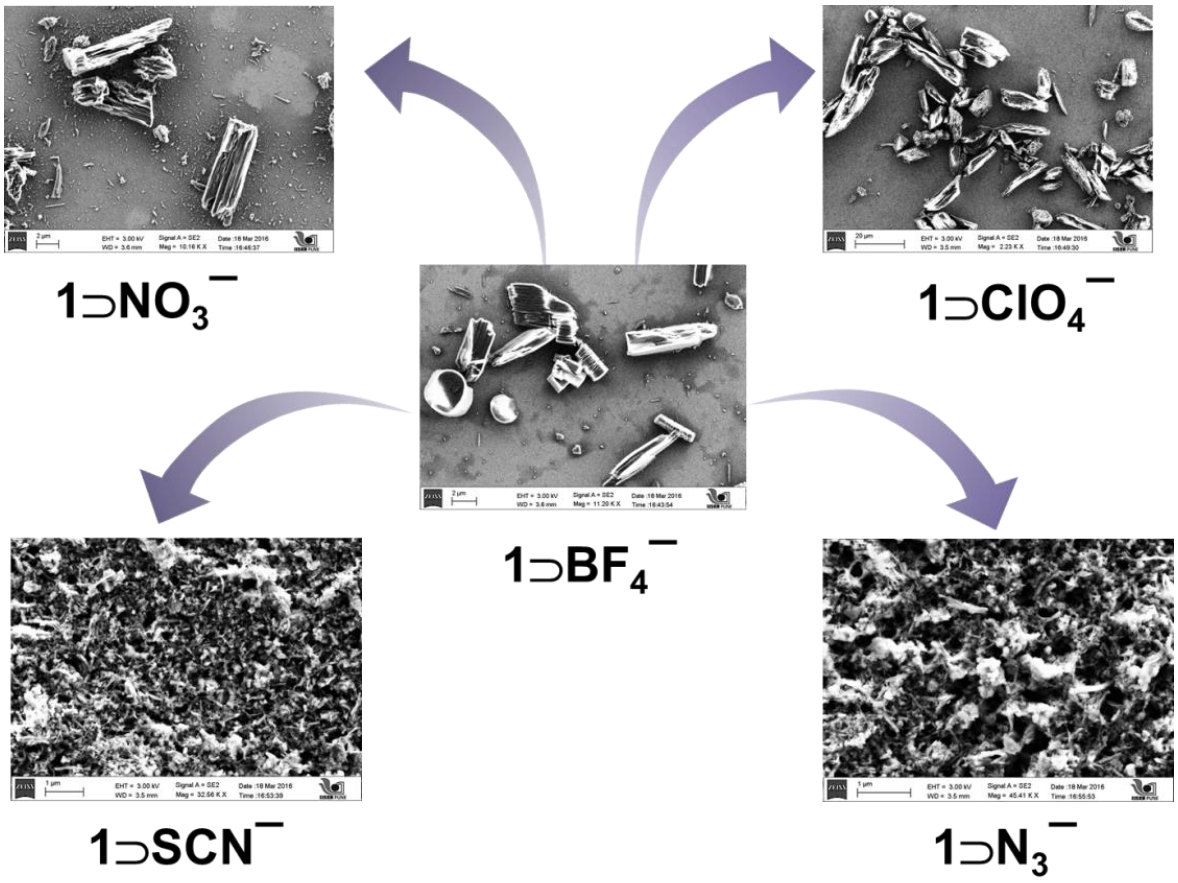

Figure 19. SEM images of $1\supset BF_4^-$ and other anion exchanged samples.

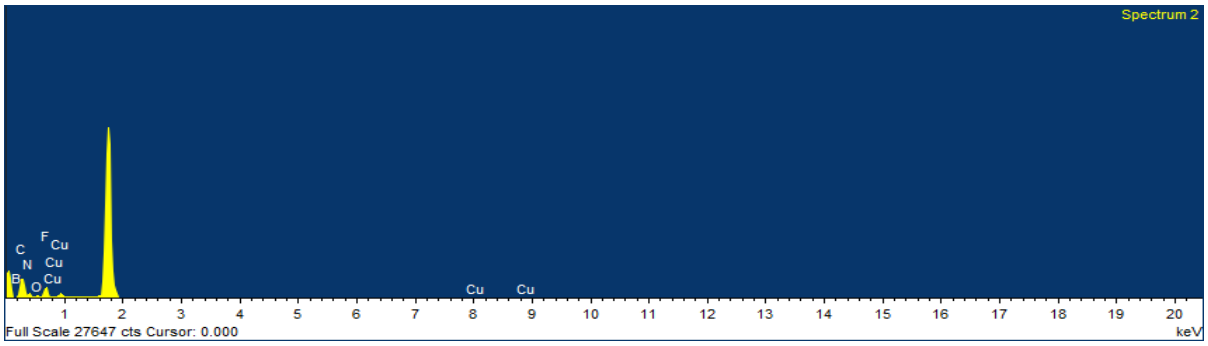

Element	Weight%	Atomic%
B K	14.05	17.63
C K	42.32	47.82
N K	20.26	19.63
O K	3.51	2.98
F K	15.36	10.97
Cu L	4.49	0.96
Totals	100.00	

Figure 20. EDX results of $1\supset BF_4^-$

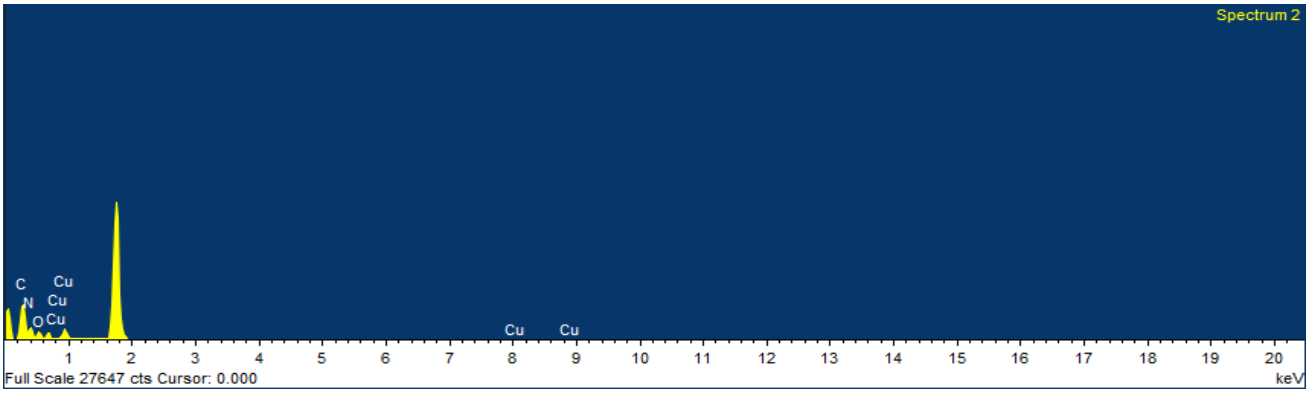

Element	Weight%	Atomic%
C K	35.11	43.02
N K	37.53	39.42
O K	16.31	15.00
Cu L	11.06	2.56
Totals	100.00	

Figure 21. EDX results of 1⊃NO_3^-

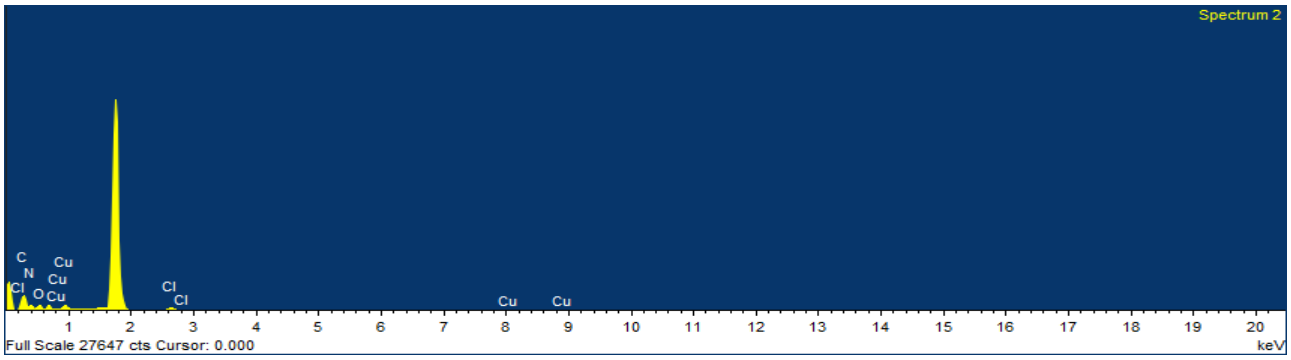

Element	Weight%	Atomic%
C K	36.64	44.91
N K	31.85	33.47
O K	20.03	18.43
Cl K	2.92	1.21
Cu L	8.56	1.98
Totals	100.00	

Figure 22. EDX results of 1⊃ClO_4^-

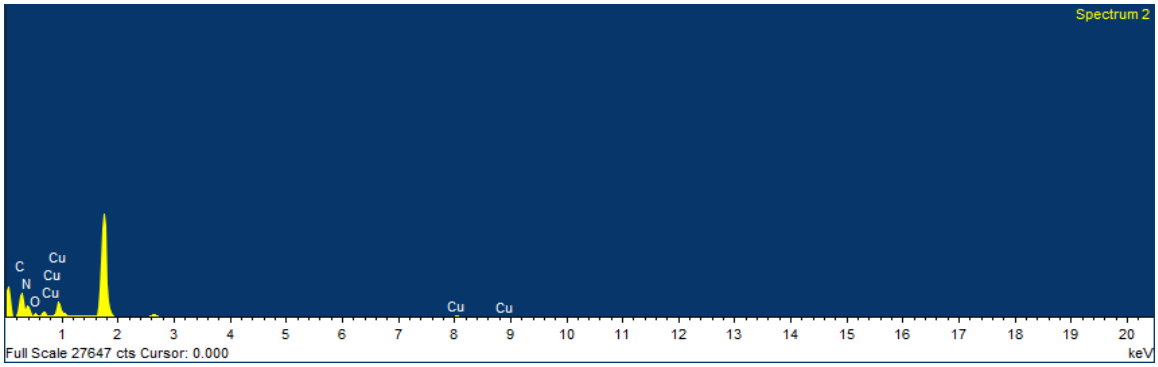

Element	Weight%	Atomic%
C K	32.40	41.25
N K	42.35	46.23
O K	9.00	8.61
Cu L	16.26	3.91
Totals	100.00	

Figure 23. EDX results of 1⊃N_3^-

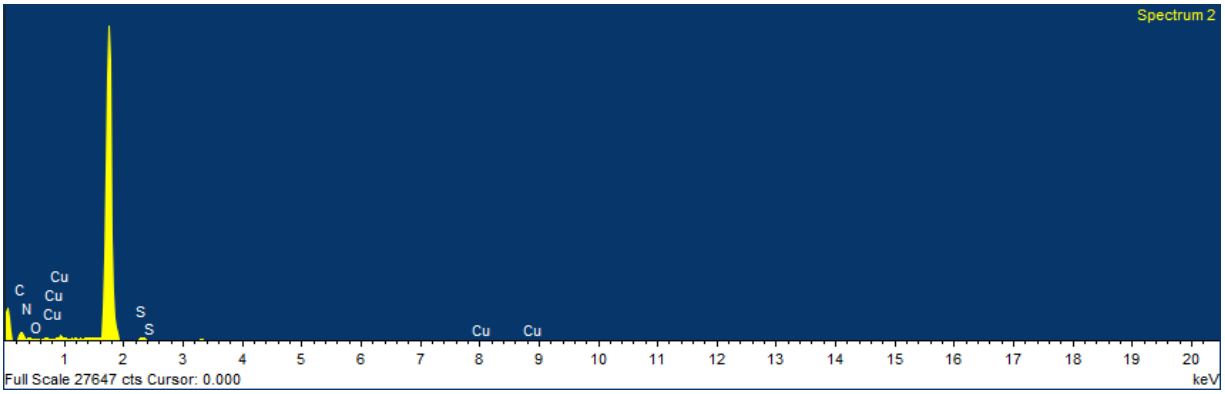

Element	Weight%	Atomic%
C K	35.80	44.25
N K	38.70	41.03
O K	11.30	10.49
S K	3.97	1.84
Cu L	10.23	2.39
Totals	100.00	

Figure 24. EDX results of 1⊃SCN^-

Owing to the presence of the open metal sites in the compound $1'\supset BF_4^-$ and the presence of lewis basic sites, phenolic oxygen and the nitrogen atoms of the ligand in the compound, the gas adsorption measurements at low temperatures for both CO_2 and N_2 shows a clear separation in the adsorption profile (Fig. 25). This is mainly due to the polar quadruple interactions of the CO_2 molecules with the framework lattice. Such type of separation is a key factor in carbon capture & storage (CCS) and clean energy applications and holds great promise for the future in chemical industries.

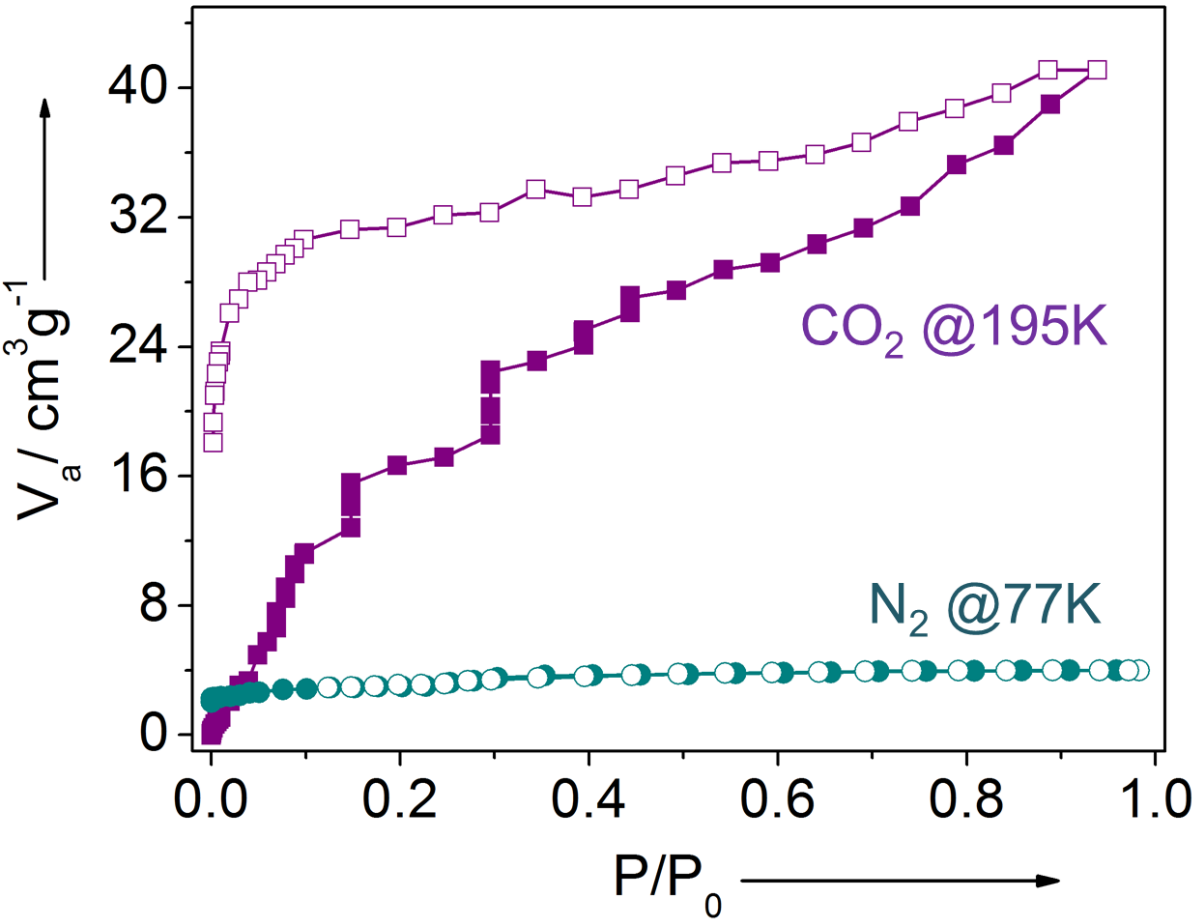

Figure 25.Low temperature gas (CO_2 and N_2) adsorption isotherms of the compound $1'\supset BF_4^-$.

Conclusion:

In conclusion, we synthesized a one dimensional co-ordination polymer resulting from a triazine core based N-donor ligand and $Cu(BF_4)_2$. The as-synthesized compound had both free and coordinated BF_4^- inside the framework, which underwent colorimetric anionic behaviour, when exchanged with NO_3^-, ClO_4^-, N_3^- and SCN^- depending on the size, shape and co-ordination tendency. The selectivity of the anions, taking equimolar binary mixtures of the anions at a time were also studied, resulting the affinity of the anions towards the framework as: N_3^->SCN^->NO_3^->ClO_4^-. Also, the compound owing to the presence of electron rich lewis basic sites shows a selective uptake of CO_2 over N_2. Such type of multifunctional materials has been a key theme of research for the people working in academia & industries and development of new materials showing such multifunctional behaviour is desirable.

References:

1. Zhou, H.-C.; Long, J. R.; O. M. Yaghi, O. M. Introduction to Metal−Organic Frameworks *Chem. Rev.* **2012**, *112*, 673 – 674. b) Karmakar, A.; Kumar, N.; Samanta, P.; Desai, A. V.; Ghosh, S. K., A post-Synthetically Modified MOF for Selective and Sensitive Aqueous-Phase Detection of Highly Toxic Cyanide Ions *Chem. Eur. J.* **2016**, *22*, 864-868. c) Nagarkar, S. S.; Joarder, B.; Chaudhari, A. K.; Mukherjee, S.; Ghosh, S. K. Highly Selective Detection of Nitro Explosives by a Luminescent Metal–Organic Framework *Angew. Chem. Int. Ed.* **2013**, *52*, 2881 – 2885.

2. a) McKinlay, C.; Morris, R. E.; Horcajada, P.; Ferey, G.; Gref, R.; Couvreur, P.; Serre, C. BioMOFs: metal-organic frameworks for biological and medical applications. *Angew. Chem. Int. Ed.* **2010**, *122*, 6400 – 6406. b) Lee, J. Y.; Farha, O. K.; Roberts, J., Scheidt, K. A.; Nguyen, S. T.; Hupp, J. T. Metal–organic framework materials as catalysts. *Chem. Soc. Rev.* **2009**, *38*, 1450 – 1459. c) Li, G.; Yu, W.; Cui, Y. A. Homochiral Nanotubular Crystalline Framework of Metallomacrocycles for Enantioselective Recognition and Separation. *J. Am. Chem. Soc.* **2008**, *130*, 4582 –4583. d) Uemura, T.; Yanai, N.; Kitagawa, S. Luminescent metal–organic frameworks *Chem. Soc. Rev.*, **2009**, *38*, 1228 – 1236.

3. Manna, B.; Desai, A. V.; Kumar, N.; Karmakar A.; Ghosh, S. K. Single crystal-to-single-crystal transformation of an anion exchangeable dynamic metal–organic framework. *CrystEngComm.* **2015**, *17*, 8796-8800.
4. Maji, T. K.; Matsuda, R.; Kitagawa, S. A flexible interpenetrating coordination framework with a bimodal porous functionality. *Nat. Mater.* **2007**, *6*, 142 –148.

5. Fei, H.; Bresler, M. R.; Oliver, S. R. J. A New Paradigm for Anion Trapping in High Capacity and Selectivity: Crystal-to-Crystal Transformation of Cationic Material. *J. Am. Chem. Soc.* **2011**, *133*, 11110-11113.
6. Fei, H.; Han, C. S.; Robins, J. C.; Oliver, S. R. J. A Cationic Metal–Organic Solid Solution Based on Co(II) and Zn(II) for Chromate Trapping *Chem. Mater.* **2013**, *25*, 647-652.

7. Coronado, E.; Espallargas, G. M. Dynamic magnetic MOFs. *Chem.Soc.Rev.* **2013**, *42*, 1525—1539.

8. a) Beer, P. D.; Gale, P. A. Anion Recognition and Sensing: The State of the Art and Future Perspectives. *Angew. Chem., Int. Ed.* **2001**, *40*, 486-516. b) Ma´n˜ez, R. M.; Sanceno´n, F. Fluorogenic and Chromogenic Chemosensors and Reagents for Anions. *Chem. Rev.* **2003**, *103*, 4419-4476.
9. a) Gong, Y.; Qin, J. B.; Wu, T.; Li, J. H.; Yang, L.; Cao, R. Synthesis, structural characterization and anion-sensing studies of metal (II) complexes based on 3,3 ¢,4,4 ¢-oxydiphthalate and N-donor ligands. *Dalton Trans*. **2012**, 41, 1961 –1970. b) Palacios, M. A.; Nishiyabu, R.; Marquez, M.; Anzenbacher, P. Supramolecular Chemistry Approach to the Design of a High-Resolution Sensor Array for Multianion Detection in Water. *J. Am. Chem. Soc.* **2007**, *129*, 7538 –7544.

10. Alhamami, M.; Doan, H.; Cheng, C.-H. A Review on Breathing Behaviors of Metal-Organic-Frameworks (MOFs) for Gas Adsorption. *Materials*. **2014**, *7*, 3198-3250.
11. Ma, J. P.; Yu, Y.; Dong, Y. B. Fluorene-based Cu(II)-MOF: a visual colorimetric anion sensor and separator based on an anion-exchange approach. *Chem. Commun.* **2012**, *48*, 2946-2948.
12. Manna, B.; Desai, A. V.; Ghosh, S. K. Neutral N-donor ligand based flexible metal– organic frameworks. *Dalton Trans.* **2016**, *45*, 4060–4072.
13. Karmakar, A.; Desai, A. V.; Ghosh, S. K. Ionic metal-organic frameworks (iMOFs): Design principles and applications. *Coord. Chem. Rev.* **2016**, *307*, 313-341.
14. White, C. M.; Smith, D. H.; Jones, K. L.; Goodman, A. L.; Jikich, S. A.; LaCount, R. B.; DuBose, S. B.; Ozdemir, E.; Morsi, B. I.; Schroeder, K. T. Sequestration of Carbon Dioxide in Coal with Enhanced Coalbed Methane Recovery A Review. *Energy Fuels*. **2005**, *19*, 659.
15. Seoane, B.; Coronas, J.; Gascon, J.; Benavides, M. E.; Karvan, O.; Caro, J.; Kapteijn, F.; Gascon, J.Metal–organic framework based mixed matrix membranes: a solution for highly efficient CO_2 capture? *Chem. Soc. Rev.* **2015**, *44*, 2421-2454.

16. Chen, Y.–Q.; Li, G.-R.; Chang, Z.; Qu, Y.–K.; Zhang, Y.-H.; Bu, X.-H. A Cu(I) metal–organic framework with 4-fold helical channels for sensing anions. *Chem. Sci.* **2013**, *4*, 3678–3682.
17. a) Kong, L.; Zou, R.; Bi, W.; Zhong, R.; Mu, W.; Liu, Jia; Hana, R. P. S.; Zou, R. Selective adsorption of CO2/CH4 and CO2/N2 within a charged metal–organic framework. *J. Mater. Chem. A*. **2014**, *2*, 17771–17778. b) Li, J.-R., Ma, Y.; McCarthy, M. C.; Sculley, J.; Yu, J.; Jeong, H.-K.; Balbuena, P. B.; Zhou, H.-C. Carbon dioxide capture-related gas adsorption and separation in metal-organic frameworks. *Coordination Chemistry Reviews*. **2011**, *255*, 1791–1823.
18. Karmakar, A.; Desai, A. V.; Manna, B.; Joarder, B.; Ghosh, S. K. An Amide Functionalized Dynamic Metal–Organic Framework Exhibiting Visual Colorimetric Anion Exchange and Selective Uptake of Benzene over Cyclohexane. *Chem. Eur. J.* **2015**, *21*, 7071 – 7076.
19. *SAINT Plus*, (Version 7.03); Bruker AXS Inc.: Madison, WI, **2004**.
20. G. M. Sheldrick, *SHELXTL*, *Reference Manual*: version 5.1: Bruker AXS; Madison, WI, **1997**.
21. G. M. Sheldrick, *Acta Crystallogr. Sect. A* **2008**, 112 –122.
22. WINGX version 1.80.05 Louis Farrugia, University of Glasgow.
23. A. L. Spek, (**2005**) PLATON, *A Multipurpose Crystallographic Tool*, Utrecht University, Utrecht, The Netherlands.
24. Azarifar, D.; Zolfigol, M. A.; Forghaniha, A. A Convenient Method for the Preparation of Some New DEerivatives of 1,3,5- *s*-Triazine Under Solvent Free Condition. *Heterocycles*. **2004**, *63*, 1897 –1901.
25. Goodgame, D. M. L.; Grachvogel, D. A.; Williams, D. J. A New Type of Metal-Organic Large-Pore Zeotype. *Angew. Chem. Int. Ed.* **1999**, *38*, 153-156.

Chapter 2

Syntheses and Characterization of small pores Al based MOF nanoparticles for gas separation in mixed matrix membranes

(This part of work was done at Institut Lavoisier de Versailles (ILV), UVSQ, Versailles (France), under the guidance of Dr. Christian Serre and Dr. Clemence Sicard.)

Introduction

The increasing emissions of greenhouse gases and its major impact on global warming is a main concern of depleting environment and climate change internationally. It leads to significant capture and separation of CO_2 from other gases to overcome this critical global climate change.[1] The major source of CO_2 are industrial flue gases and burning of fossil fuels. Several strategies have been attempted to capture the CO_2 from the flue gases. Chemical adsorption of mono-ethanol amine (MEA) and di-ethanol amine (DEA) aqueous solution is one of the most successful attempts, used industrially. However, this process requires a considerable amount of energy and involves amines and noxious solvents, which are not environment friendly.[2] Therefore, more efficient, less energy requiring and environment friendly capture technologies need to be introduced.

Membrane-based gas separation attracted more industries and research & development sectors in recent days. It dominates over other separation technologies such as adsorption, amine absorption and cryogenic separation due to its less energy requiring and environment friendly speciality.[2, 3] There are many reports of membranes, constituting polymer based and inorganic membranes till date. Both types of membranes have their own advantages and disadvantages. Mixed matrix membranes (MMMs) eradicate the challenges caused by both types of membranes, showing ease of reproducibility, which lacks in the inorganic membranes and having mechanical, thermal and physical properties for harsh environment conditions, which lack in polymer-based membranes and thus are better suited for gas separation applications.[3]

MMMs comprise of inorganic fillers such as zeolites, carbon nanotubes, and metal organic frameworks (MOFs) dispersed in the matrix designed by organic polymers.[4, 5] Since, MOFs are constitute of metal and organic linkers, they possess an hybrid nature of both inorganic and organic phases, and hence could excel over other fillers showing better affinity with the polymeric matrix.[6]

MMMs should be thin membranes, thus it is necessary to use MOFs particles at the nanometric scale in order to achieve a good dispersion of the fillers into the polymeric matrices, good colloidal dispersion need to be obtained.[7] Some MOFs are

known to be good candidates for gas separations. This reasons our target to synthesize nanoparticles of MOFs.

MIL-69(Al) ($Al(OH)(O_2C–C_{10}H_6–CO_2)·H_2O$) (MIL = Material Institute Lavoisier)(Figure 1) is a MOF, first reported by T. Loiseau et al. that shows a promising potential to be used as a filler for MMMs for CO_2 capture and separation. Indeed, MIL-69 is an isoreticularphase of MIL-53(Al)-NH_2 that is known to be an efficient filler for MMMs for CO_2/ N_2separation.[8, 9] In MIL-69, the terephthalate ligands of MIL-53 are replaced by naphthalenedicarboxylate (ndc) ligands, leading to stronger π-π interactions and thus a reduced flexibility that highly improves selectivity to CO_2 in a mixture of CO_2/N_2.[10] MIL-69(Al) (Fig. 1) is hydrothermally synthesized at 210 ^oC for 16 h, using 2,6-naphthalenedicarboxylic (ndc) acid, aluminium nitrate and KOH, with approximate particle size of 1 µm.[11] Thus, this defines our target to synthesize nanoparticles of MIL-69 for CO_2 separation.

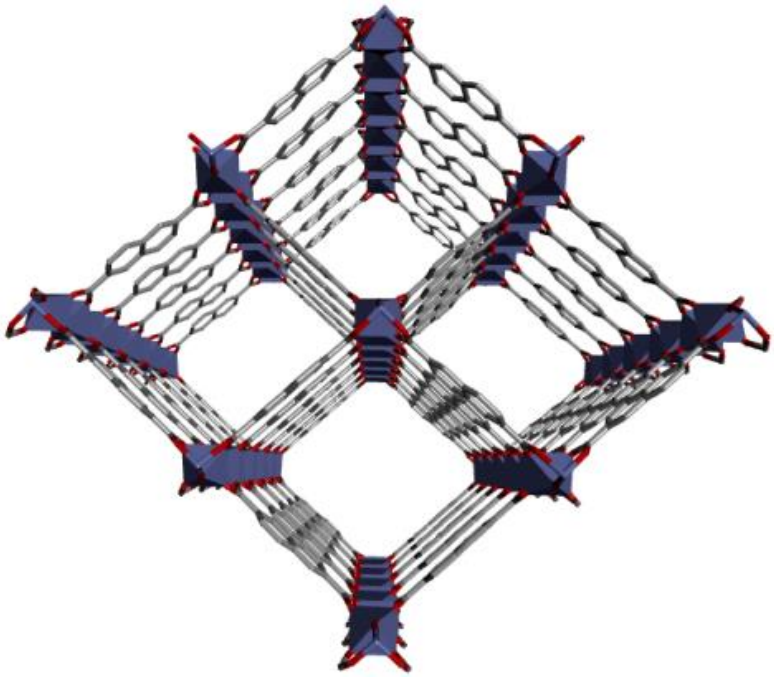

Figure 1: Perspective view of the structure of MIL-69

Several synthetic routes such as hydrothermal, microwave and reflux synthesis with varied reaction time, concentration of ligand, base and various solvents combinations were studied in Institut Lavoisier de Versailles (ILV), UVSQ, Versailles (France) prior to this work.

Experimental Section

Materials: All reagents and solvents were commercially available and were used without any further purification.

Synthesis

Hydrothermal Synthesis - Compound 1

MIL-69(Al) was hydrothermally synthesized following the procedure previously reported by T. Loiseau et al.[11] Briefly, 2,6-ndc (0.3783 g, 1.75 mmol) was dissolved in 3 mL H_2O and added to a 25 mL Teflon bomb followed by addition of KOH (0.2440 g, 4.35 mmol) in 2 mL H_2O, and finally $Al(NO_3)_3.9H_2O$ (1.314 g, 3.5 mmol) was added to the vessel. The solution mixture was stirred for 4-5 minutes and then kept in an oven for 16 hours at 210^oC. The product was filtered and washed with water and allowed to dry at room temperature.

Reflux synthesis

Reflux synthesis is well known, very easy to perform and easily transferable to large scale synthesis which is another key aspect of this project. Hence, this synthesis was preferred, in order to facilitate the scale up of the resulted compound. We, first reproduce the best synthesis developed in ILV,UVSQ, Versailles (France), and then varied various reaction conditions (concentrations, protocol,..)**.**

Standard concentration: C_{lig} = 0.1 g/ mL- Compound 2

2,6-ndc (0.4324 g, 2 mmol), NaOH (0.19 g, 4.75 mmol) and $Al(NO_3)_3.9H_2O$ (1.5 g, 4 mmol) were added to a 100 mL round bottom flask, followed by addition of 10 mL of N,N-dimethyl formaldehyde (DMF) and H_2O each. The reaction mixture in the flask was stirred under reflux condition for 5 hours. After the completion of reaction, the products were filtered, and washed with DMF, stirring at 50^oC for 5 hours. The washed product was filtered again and finally the resulting powder was calcined for 16 h at 200^oC to remove the DMF trapped within the pores of the MOF.

Increasing reactants Concentrations: C_{lig} = 0.35 g/ mL- Compound 3

Reflux synthesis with increasing reagents concentration was tried in order to diminish the particle size. 2,6-ndc (1.513 g, 7 mmol), NaOH (0.66 g, 16.625 mmol) and $Al(NO_3)_3.9H_2O$ (5.25 g, 14 mmol) were added to a 100 mL round bottom flask, followed by addition of 10 mL of DMF and H_2O each. The remaining procedures followed were the same as the standard reflux synthesis.

This reaction was also monitored in-situ by pipetting out some reaction mixture solutionat different time intervals (at 30 min, 1 hour and 2 hour).

Synthesis with green solvent- Sulfolane- Compound 4

In order to perform environment friendly synthesis, we tried to replace DMF by a less toxic solvent: sulfolane, which has similar physico-chemical properties as DMF but lower toxicity. The reaction procedures remained identical to the higher concentration one (C_{lig} = 0.35 g/ mL, compound 3), except the solvent ratio. Since, the ligand solubility in sulfolane is lower than in DMF, a mixture 3:1 sulfolane (15 mL): H_2O (5 mL) was used. Using sulfolane for the washing step was also tested.

Addition dropwise of the metal salt- Compound 5

2,6-ndc (1.513 g, 7 mmol), NaOH (0.66 g, 16.625 mmol) were added into a 100 mL round bottom flask, followed by addition of 10 mL of DMF and 5 mL H_2O each. Solution of $Al(NO_3)_3.9H_2O$ (5.25 g, 14 mmol) was dissolved in 5 mL water and added dropwise to the reaction mixture after refluxing for an hour and then the reaction was allowed to run for another 4 hours. The resulted compounds were centrifuged and the obtained products were washed with DMF to remove the unreacted ligands. Finally the pure products were obtained by centrifugation and calcined.

Physical measurements

The different compounds were characterized by Powder X-ray diffraction (PXRD), Infra-Red spectroscopy (IR), Thermal Gravimetric Analyses (TGA), Scanning Electron Microscopy (SEM), Transmission Electron Microscopy (TEM) and Dynamic Light Scattering (DLS)

Powder X-ray diffraction (PXRD)

Powder X-ray diffraction data of all the synthesized compounds were collected at 293 K on a Siemens D-5000 diffractometer by using CuKa radiation k = 1.5418 Å.

Thermogravimetric analyses (TGA)

Thermogravimetric analyses were performed on a TA-instrument 2050 under O_2atmosphere between room temperature and 700 ^oC with a heating ramp of 3^oC/min,**.**

Fourier Transform Infra-red spectroscopy(FT-IR)

Infra-red spectra were recorded with a Thermo Nicolet spectrometer (Thermo, USA) from 4000-400 cm^{-1}.

Dynamic light scattering (DLS)

Particle size was monitored by Dynamic Light Scattering (DLS) on a Zetasizer Nano (Malvern Instruments). Samples were prepared by dispersing at 0.033 g/ L of nanoparticles (NPs) in ethanol by using an ultrasound tip (30% amplitude for 30 sec; Digital Sonifer 450, Branson).

Scanning Electron Microscopy (SEM)

Samples were imaged using a Jeol JSM-7001F microscope using gold coated samples equipped with an energy-dispersive X-ray (EDX) spectrometer with a X-Max SDD (Silicon Drift Detector) by Oxford.

Results and discussions:

PXRD studies

Compound 1 (hydrothermal synthesis)

The product was characterized by Powder X-ray diffraction (PXRD) and hence confirmed the formation of MIL-69, matching the characteristic peaks (Fig. 2) of the simulated patterns.

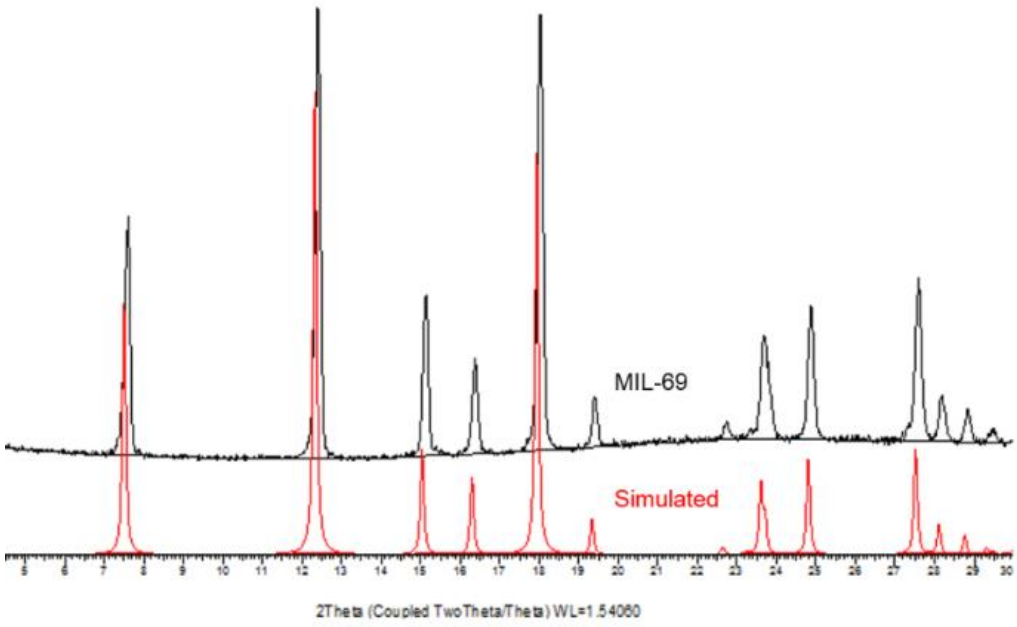

Figure 2: PXRD patterns of MIL-69 (as synthesized- black) and simulated (red).

Compound 2 (standard reflux synthesis)

The formation of MIL-69(Al) was confirmed by PXRD with peaks of the synthesized product as shown in the figure 3, matching the characteristic peaks of the simulated pattern. In the as-synthesised product (before washing), the first peak at 2θ= 7.5° is doubled and extra peak at 2θ = 14.2°is presented, most likely due to a variation in the pores opening due to the presence of solvent within the pores, that vanishes in calcined product where solvent molecules have been removed from the pores.

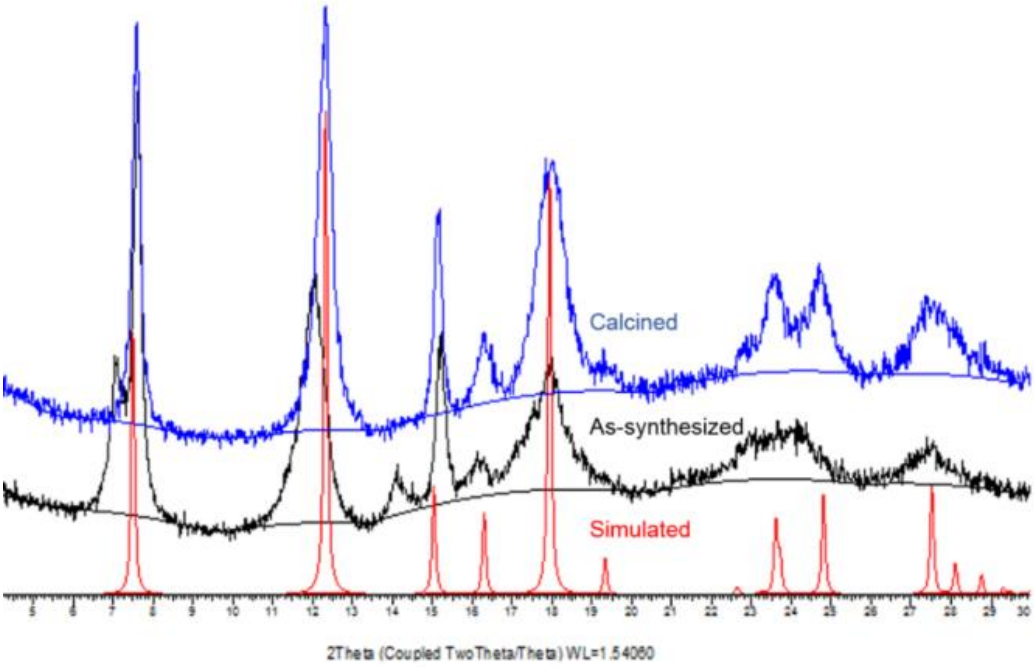

Figure 3: PXRD patterns of the simulated (red) MIL-69, as-synthesized (black) and calcined (blue) products.

Compound 3: Higher concentration and *In-situ* crytallisation studies (Varying the reaction time)

The PXRD patterns (Fig. 4) confirmed the formation of MIL-69 even after 30 minutes, even if some unreacted ligand was still present (peak at 2θ = 26.8°)but was easily removed by washing with DMF for 5 hours at 50 ^{o}C. The peaks width did not seem to be larger at lower reaction time, and thus suggesting shorter reaction time does not lead to smaller crystallite domains (Scherrer law, it is to note that due to the phase flexibility, the exact size of the crystallite domains could not be calculated accurately).

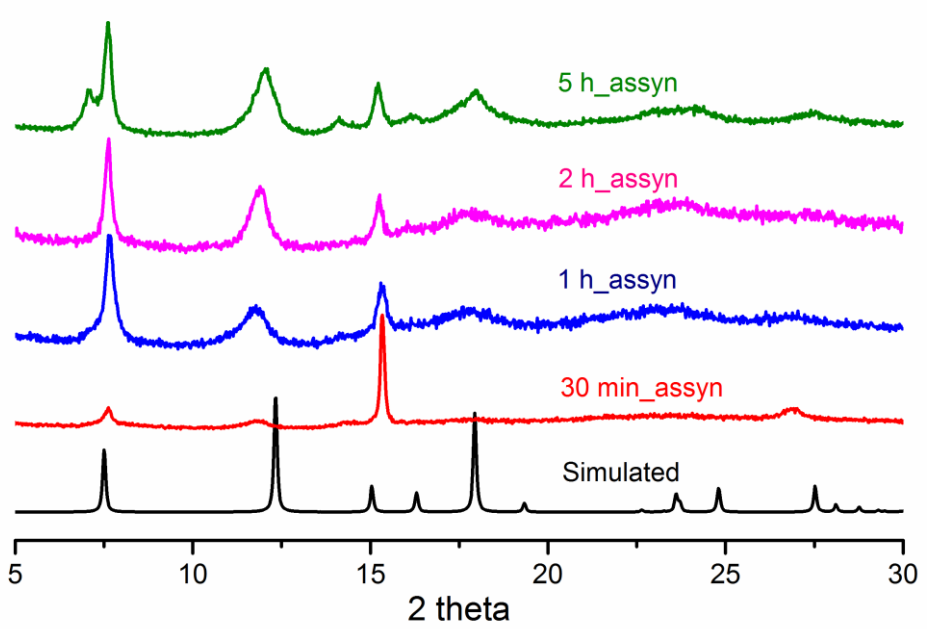

Figure 4. PXRD patterns of products at 30 min (red), 1 h (blue) and 2 h (pink) and 5 h (green).

Compound 4:

The PXRD patterns showed the characteristic peaks of MIL-69 (Fig. 5). The remaining ligand was not removed by sulfolane wash but was easily removed by a DMF wash.

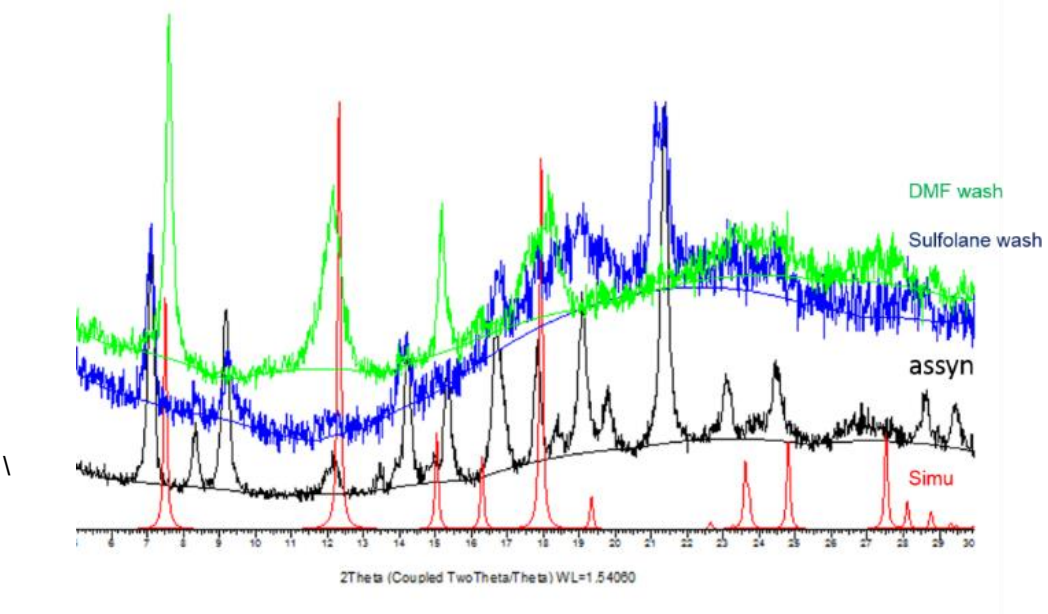

Figure 5. PXRD patterns of the as-synthesized product (black), product after sulfolane wash (blue) and the product after DMF wash (green). The product with DMF wash (green) gives pure product, as the PXRD peaks match with the characteristic peaks of the simulated patterns (red).

Compound 5:

The PXRD patterns show the characteristic peaks of MIL-69 and hence confirmed the formation of the compound MIL-69. The large peaks width suggest the formation of small crystallite domains.

Fourier Transform Infrared Spectroscopy (FT-IR):

The infrared spectrum of the compound 2 also confirmed the formation of the desired product (Fig. 6), showing the characteristic bands of the MIL-69 (hydrothermal). This is also supported by the absence of the vibration band at approximately 1700 cm^{-1} that corresponds to free carboxylic group, leaving hardly any trace of unreacted ligand. IR spectra of compounds 3, 4 and 5 also resemble with the IR spectra of the compound 2.

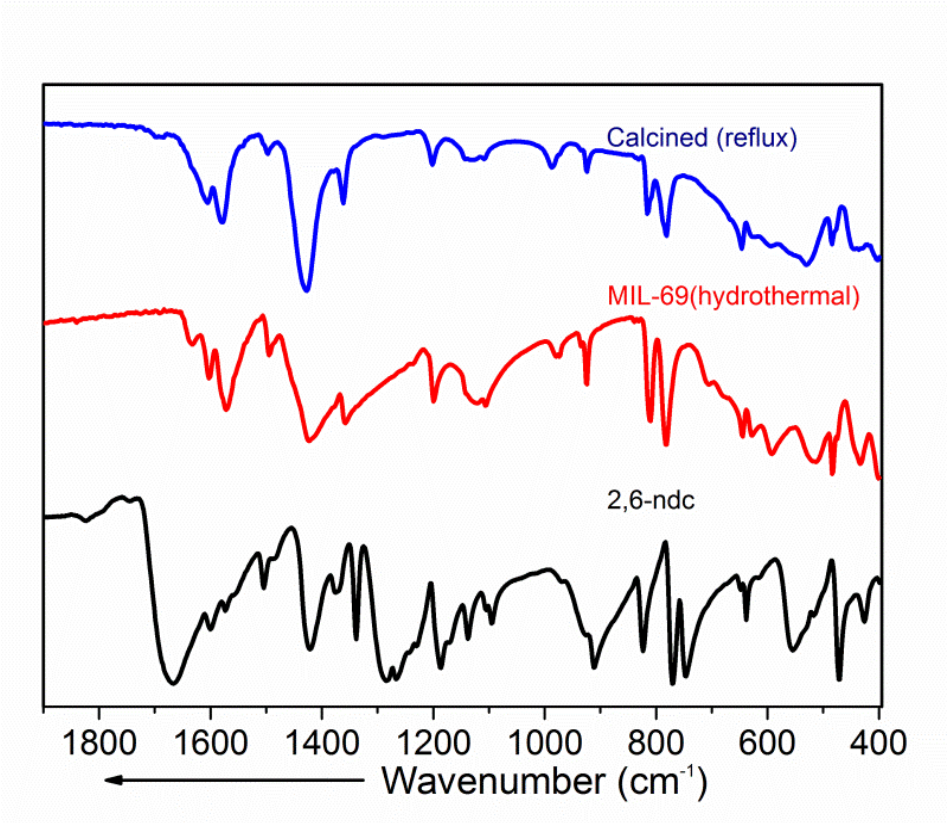

Figure 6. Infra-red spectrum of calcined product through reflux synthesis (blue), MIL-69 through hydrothermal synthesis (red) and the ligand (2,6-ndc) (black).

Thermogravimetric analysis (TGA):

The TGA of the products are as shown in figure 7.

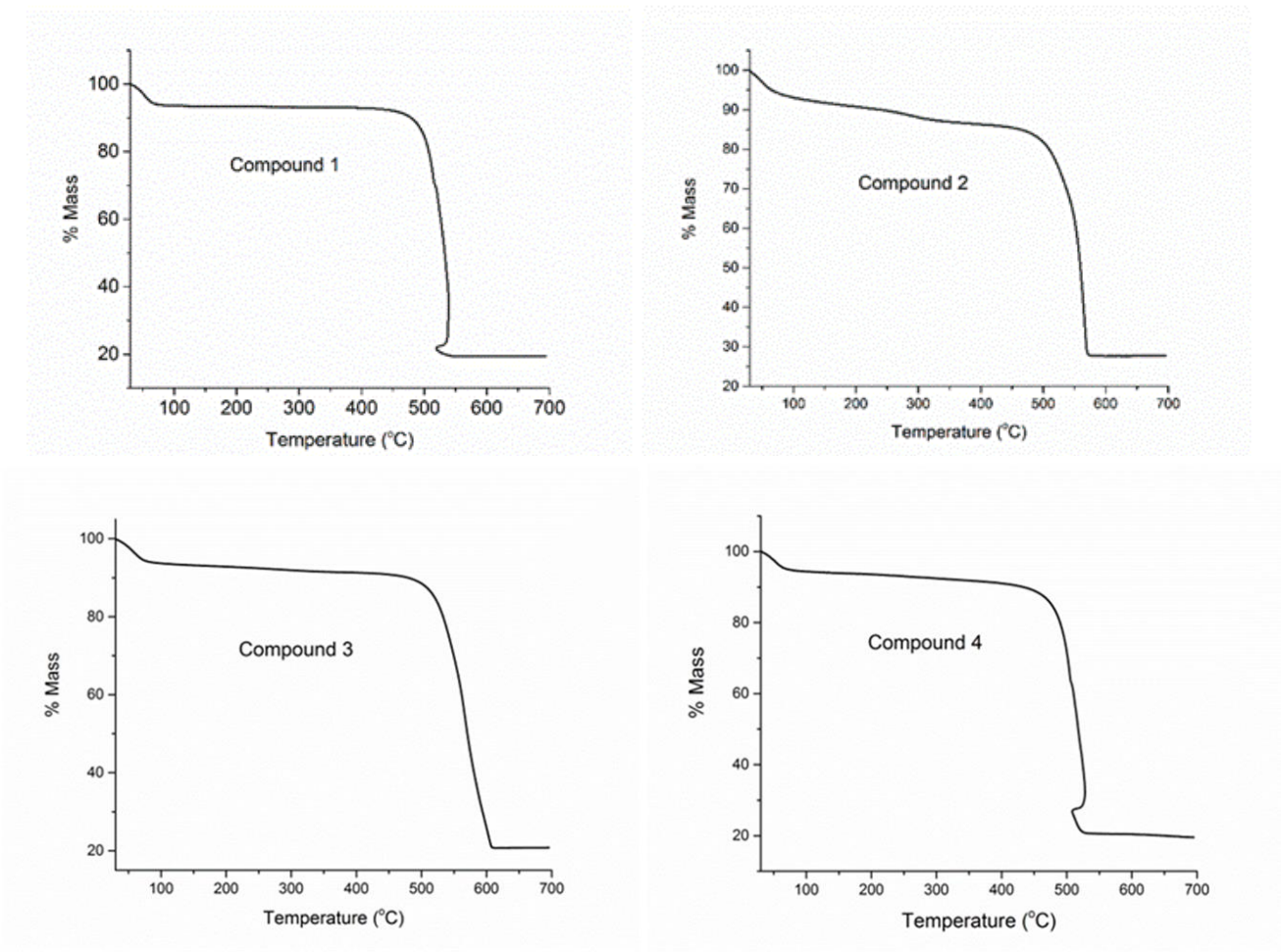

Figure 7: TGA curves of compounds 1, 2 3 & 4.

The first weight loss corresponds to removal of the free solvent molecules (H_2O/ DMF). Then, the organic framework starts to degrade at approximately 450$^oC$and finally formation of Al_2O_3 is observed. The different percentages of weight losses are presented in table 1 and showing that all the compounds, except compound 2, have almost comparable results with the calculated one, suggesting that a minimal amount of oxide has been former during the synthesis. The curve of compound 2 show a second weight loss around 250^oC, that may be due to the presence of solvent molecules still present inside the pores of the framework.. Also, compound 2 showed a higher amount of residue, suggesting the presence of aluminium oxide during the synthesis.

	Compound 1	Compound 2	Compound 3	Compound 4	Calculated
H_2O loss	6.1 %	5.8 %	6.2 %	5.3 %	6.9 %
Organic loss	72.4 %	66.5 %	70.1 %	70.3 %	74 %
Residue	19.5 %	27.7 %	20.8 %	20.4 %	19.1 %

Table 1: Comparison of the TGA data of all compounds 1-4.

SEM images

SEM images of different synthesized compounds are depicted in the figure 8, starting from a-e and their corresponding sizes are presented in the table 2. The hydrothermally synthesised compound 1 has particles of more than 1 µm in size not in agreement with the requirement of sub-micrometric MOFs particles to be used as inorganic fillers in MMMs. All the compounds synthesised under reflux conditions are below 400 nm in size but very polydispersed in size. It is to note that higher reagents concentration (compound 3) seems to lead to more crystalline particles than less concentrated synthesis (compound 2). As suggested by the XRD, shorter reaction time did not yielded neither smaller particle, nor more homogeneous.

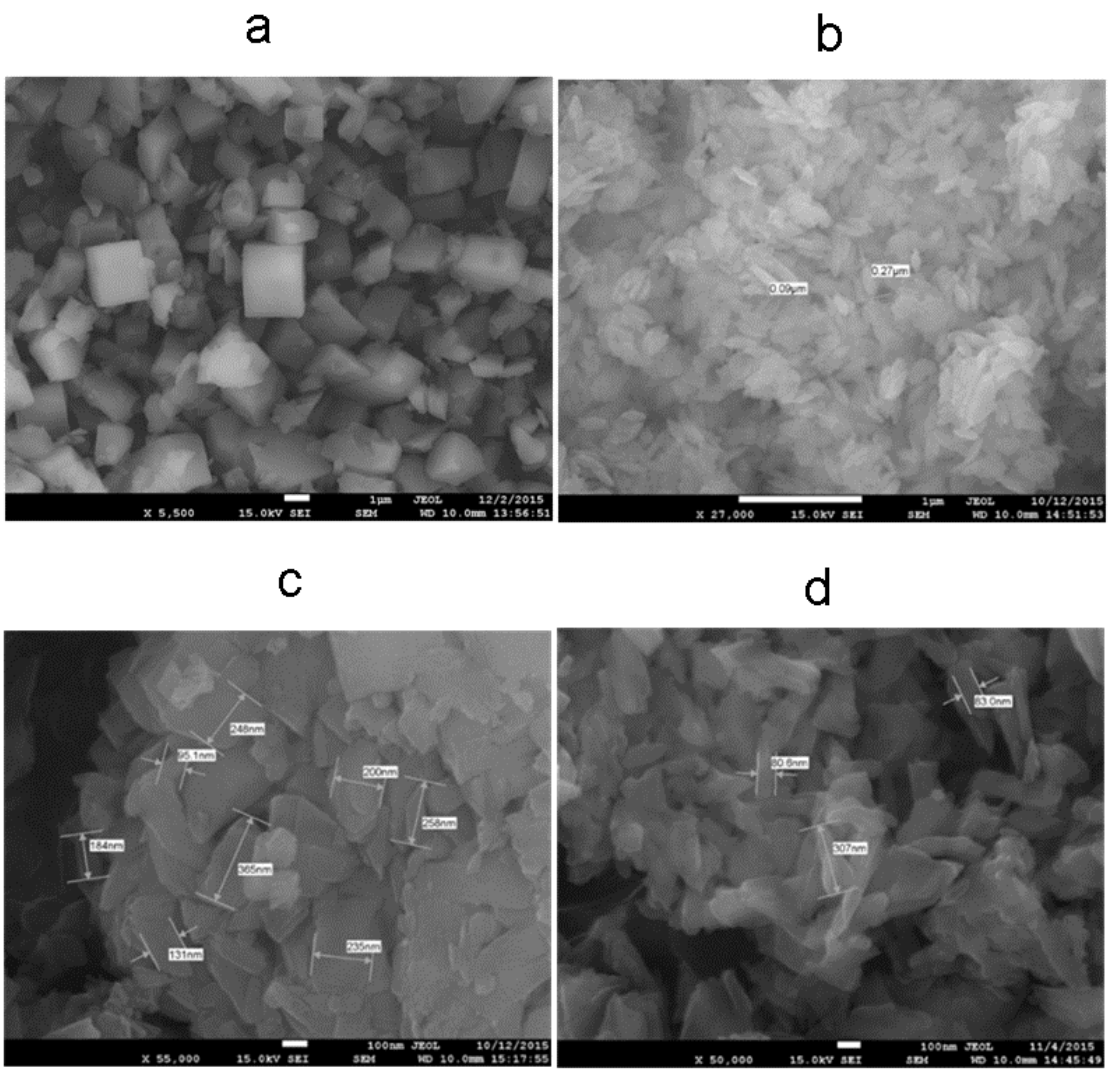

Table 2.

	Compounds		Size
a	Compound 1		> 1 µm
b	Compound 2		90-300 nm
c	Compound 3		95-370 nm
d	Compound 3	Monitored at 30 min	80-350 nm
e		Monitored at 1 h	68- 300 nm

Figure 8. SEM images of compounds 1, 2 & 3 are represented in a, b & c respectively. SEM images of the compound 3 monitored at 30 min and 1 h are in d & e respectively and Table 2, representing the corresponding sizes of the compounds 1, 2 & 3.

TEM images

TEM image of the compound synthesized at standard concentration (figure 9 a) are in agreement with the SEM images, showing particles, ranging from 80-300 nm and not well define shape. The TEM image of the compound synthesized at higher concentration (figure 9 b), shows the size of the particles ranging from 80-370 nm with a well define shape. The TEM image of the compound synthesized using Sulfolane instead of DMF shows the particle size ranging from 100-200 nm. The TEM image of the compound synthesized involving the addition of the metal salt after an hour shows the particle size ranging from 60-120 nm. In this case also, the particles were well crystallized. This synthesis gave the smaller particles. The formation of the smaller particles in this synthesis may be because of the higher control of the nucleation and growth steps, enabled by the dropwise addition of the metal.

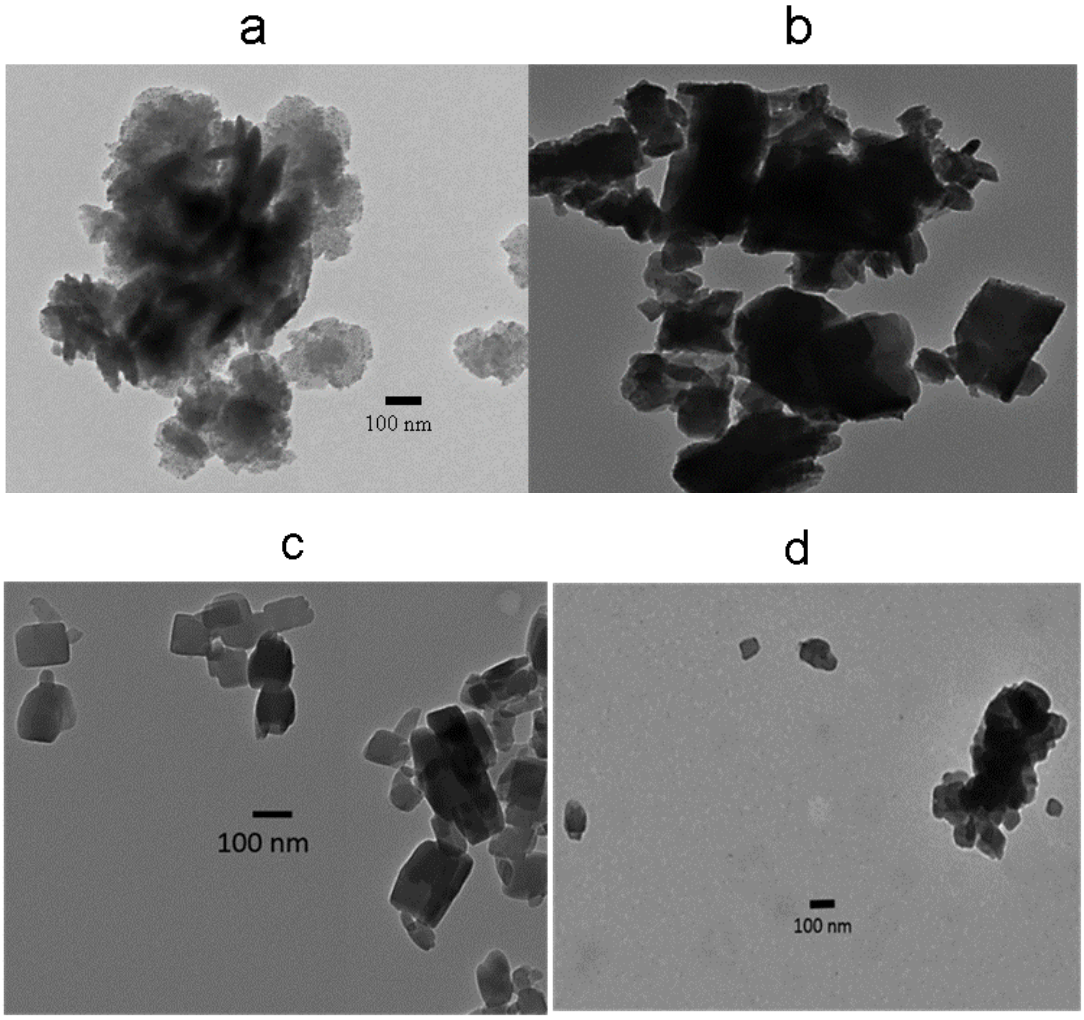

Figure 9. TEM images of compound 2, 3, 4 & 5 in a, b, c & d respectively.

Dynamic Light Scattering (DLS) measurements:

The table 3 represents the values measured. Likewise results shown by SEM & TEM images, the compound 2 is bigger in size with high polydispersivity. The compounds 4 & 5 are smaller in size and have a smaller polydispersivity index.

Compounds	Number mean	PDI
Compound 2	433 ± 30 nm	0.56
Compound 4	230 ± 40 nm	0.23
Compound 5	175 ± 23 nm	0.23

Table 3: DLS measurements of the compound 2, 4 & 5.

Conclusion:

This work was performed in the context of MOFs-based mixed matrix membranes (MMMs) for CO_2/N2 separation selectively. MIL-69 is extremely interesting among various MOFs to separate CO_2 selectively in the mixture of CO_2 and N_2. Synthesis of MIL-69 at the nanometric scale was focused to be used as inorganic fillers in MMMs. Different parameters such as reactant concentration, solvents, reaction time, sequence of addition of the reagents were tested in order to synthesize homogenous & smaller particles. Synthesis performed under reflux condition yield particles below 400 nm but polydispersed in size. Attempts to perform the synthesis in environmental friendly conditions (replacing DMF) were tested and gave smaller particles (around 200 nm). Finally by adding the aluminium salt dropwise MIL-69 of particles size 60-120 nm were obtained. The various particles are currently being tested for their gas separation properties and as MMMS fillers.

References:

1. Zhou, D. D.; He, C. T.; Liao, P. Q.; Xue, W.; Zhang, W. X.; Zhou, H. L.; Zhang, J. P.; Chen, X. M.A flexible porous Cu(II) bis-imidazolate framework with ultrahigh concentration of active sites for efficient and recyclable CO_2 capture. *Chem. Commun.* **2013**, *49*, 11728-11730.
2. Seoane, B.; Coronas, J.; Gascon, J.; Benavides, M. E.; Karvan, O.; Caro, J.; Kapteijn, F.; Gascon, J.Metal–organic framework based mixed matrix membranes: a solution for highly efficient CO_2 capture? *Chem. Soc. Rev.* **2015**, *44*, 2421-2454.
3. Bernardo, P.;Drioli, E.; Golemme, G. Membrane Gas Separation: A Review/State of the Art. *Ind. Eng. Chem. Res.* **2009**, *48*, 4638–4663.
4. Khalilpour, R.; Mumford, K.; Zhai, H.; Abbas, A.; Stevens, G.; Rubin, E. S. Membrane-based carbon capture from flue gas: a review. *J. Clean Prod.* **2015**, *103*, 286-300.
5. Zornoza, B.; Tellez, C.; Coronas, J.; Gascon, J.; Kapteijn, F.Metal organic framework based mixed matrix membranes: An increasingly important field of research with a large application potential. *MicroporMesopor Mat.* **2013**, *166*, 67-78.
6. Xin, Q.; Liu, T.; Li, Z.; Wang, S.; Li, Y.; Li, Z.; Ouyang, J.; Jiang, Z.; Wu, H. Mixed matrix membranes composed of sulfonated poly(ether ether ketone) and a sulfonated metal– organic framework for gas separation. *J. Membr. Sci.* **2015**, *488*, 67–78.
7. Chung, T. S.; Jiang, L. Y.; Li, Y.; Kulprathipanja, S.Mixed matrix membranes (MMMs) comprising organic polymers with dispersed inorganic fillers for gas separation. *Prog. Polym. Sci.* **2007**, *32*, 483–507.
8. Couck, S.; Gobechiya, E.; Kirschhock, C. E. A; Crespo, P. S., AlcaÇiz, J. J.; Joaristi, A. M.; Stavitski, E.; Gascon, J.;Freek K.; Baron, G. V.; Denayer, J. F. M. Adsorption and Separation of Light Gases on an Amino-Functionalized Metal–Organic Framework: An AdsorptionandIn Situ XRD Study. *ChemSusChem*. **2012**, *5*, 740 – 750.

9. Sabetghadam, A.; Seoane, B.; Keskin, D.; Duim, N.; Rodenas, T.; Shahid, S.; Sorribas, S.; Guillouzer, C. L.; Clet, G.; Tellez, C.; Daturi, M.; Coronas, J.; Kapteijn, F.; Gascon, J. Metal Organic Framework Crystals in Mixed-MatrixMembranes: Impact of the Filler Morphology on the Gas Separation Performance. *Adv. Funct. Mater.* **2016,** DOI: 10.1002/adfm.201505352.
10. Unpublished results obtained through the European Union Seventh Framework Programme (FP7/2007-2013) under grant agreement n° 608490, project M4CO2.
11. Loiseau, T.; Draznieks, C. M.;Muguerra, H.;Férey, G.; Haouas, M.;Taulelle, F. Hydrothermal synthesis and crystal structure of a new three-dimensional aluminum-organic framework MIL-69 with 2,6-naphthalenedicarboxylate (ndc), Al(OH)(ndc)·H2O. *C. R. Chimie*. **2005**, *8*, 765–772.